

# Journal Pre-proof

Randomized controlled-feeding study of dietary emulsifier carboxymethylcellulose reveals detrimental impacts on the gut microbiota and metabolome

Benoit Chassaing, Charlene Compher, Brittany Bonhomme, Qing Liu, Yuan Tian, William Walters, Lisa Nessel, Clara Delaroque, Fuhua Hao, Victoria Gershuni, Lillian Chau, Josephine Ni, Meenakshi Bewtra, Lindsey Albenberg, Alexis Bretin, Liam McKeever, Ruth E. Ley, Andrew D. Patterson, Gary D. Wu, Andrew T. Gewirtz, James D. Lewis



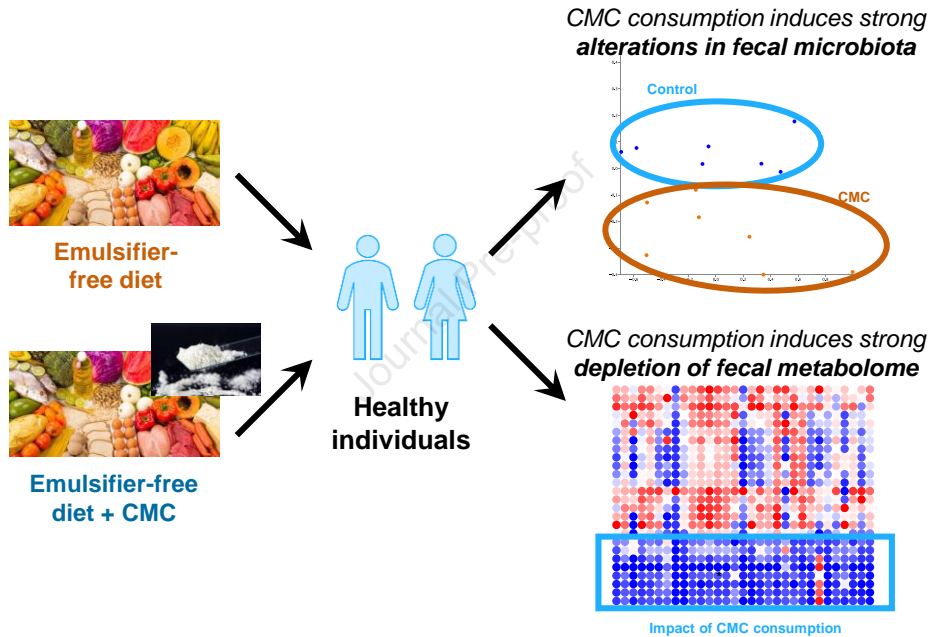
PII: S0016-5085(21)03728-8  
DOI: <https://doi.org/10.1053/j.gastro.2021.11.006>  
Reference: YGAST 64699

To appear in: *Gastroenterology*  
Accepted Date: 2 November 2021

Please cite this article as: Chassaing B, Compher C, Bonhomme B, Liu Q, Tian Y, Walters W, Nessel L, Delaroque C, Hao F, Gershuni V, Chau L, Ni J, Bewtra M, Albenberg L, Bretin A, McKeever L, Ley RE, Patterson AD, Wu GD, Gewirtz AT, Lewis JD, Randomized controlled-feeding study of dietary emulsifier carboxymethylcellulose reveals detrimental impacts on the gut microbiota and metabolome, *Gastroenterology* (2021), doi: <https://doi.org/10.1053/j.gastro.2021.11.006>.

This is a PDF file of an article that has undergone enhancements after acceptance, such as the addition of a cover page and metadata, and formatting for readability, but it is not yet the definitive version of record. This version will undergo additional copyediting, typesetting and review before it is published in its final form, but we are providing this version to give early visibility of the article. Please note that, during the production process, errors may be discovered which could affect the content, and all legal disclaimers that apply to the journal pertain.

© 2021 by the AGA Institute



1 **Randomized controlled-feeding study of dietary emulsifier carboxymethylcellulose reveals**  
2 **detrimental impacts on the gut microbiota and metabolome**

3  
4 Benoit Chassaing <sup>1, #</sup>, Charlene Compher <sup>2</sup>, Brittany Bonhomme <sup>3</sup>, Qing Liu <sup>4</sup>, Yuan Tian <sup>4</sup>,  
5 William Walters <sup>5</sup>, Lisa Nessel <sup>6</sup>, Clara Delaroque <sup>1</sup>, Fuhua Hao <sup>4</sup>, Victoria Gershuni <sup>7</sup>, Lillian  
6 Chau <sup>8</sup>, Josephine Ni <sup>9</sup>, Meenakshi Bewtra <sup>6,9</sup>, Lindsey Albenberg <sup>10</sup>, Alexis Bretin <sup>11</sup>, Liam  
7 McKeever <sup>3</sup>, Ruth E. Ley <sup>5</sup>, Andrew D. Patterson <sup>4</sup>, Gary D. Wu <sup>9</sup>,  
8 Andrew T. Gewirtz <sup>11, #</sup>, James D. Lewis <sup>3, #</sup>

9  
10 <sup>1</sup> INSERM U1016, team “*Mucosal microbiota in chronic inflammatory diseases*”, CNRS UMR  
11 8104, Université de Paris, Paris, France

12 <sup>2</sup> School of Nursing, University of Pennsylvania, Philadelphia, PA 19104, USA.

13 <sup>3</sup> Center for Clinical Epidemiology and Biostatistics, Perelman School of Medicine, University of  
14 Pennsylvania, Philadelphia, PA 19104, USA; Division of Gastroenterology and Hepatology,  
15 Department of Medicine, Perelman School of Medicine, University of Pennsylvania, Philadelphia,  
16 PA 19104, USA.

17 <sup>4</sup> Center for Molecular Toxicology and Carcinogenesis, Department of Veterinary and Biomedical  
18 Sciences, Pennsylvania State University, Pennsylvania, USA.

19 <sup>5</sup> Department of Microbiome Science, Max Planck Institute for Developmental Biology, Tübingen,  
20 Germany

21 <sup>6</sup> Center for Clinical Epidemiology and Biostatistics, Perelman School of Medicine, University of  
22 Pennsylvania, Philadelphia, PA 19104, USA.

23 <sup>7</sup> Department of Surgery, Hospital of the University of Pennsylvania, Philadelphia, PA, USA

24 <sup>8</sup> Division of Gastroenterology and Hepatology, Perelman School of Medicine, University of  
25 Pennsylvania, Philadelphia, PA 19104, USA

26 <sup>9</sup> Division of Gastroenterology, Department of Medicine, Perelman School of Medicine,  
27 University of Pennsylvania, Philadelphia, PA 19104, USA.

28 <sup>10</sup> Division of Gastroenterology, Hepatology, and Nutrition, Department of Pediatrics, Children's  
29 Hospital of Philadelphia, Perelman School of Medicine, University of Pennsylvania, Philadelphia,  
30 Pennsylvania, USA.

31 <sup>11</sup> Institute for Biomedical Sciences, Center for Inflammation, Immunity and Infection, Digestive  
32 Disease Research Group, Georgia State University, Atlanta, GA, USA

33

34 **# Corresponding Authors:**

35 - Benoit Chassaing, Ph.D.

36 INSERM, U1016, team “Mucosal microbiota in chronic inflammatory diseases”, Paris,  
37 France

38 E-Mail: [benoit.chassaing@inserm.fr](mailto:benoit.chassaing@inserm.fr)

39

40 - Andrew T Gewirtz, Ph.D.

41 Center for Inflammation, Immunity and Infection, Institute for Biomedical Sciences,  
42 Georgia State University, Atlanta, GA

43 E-Mail: [agewirtz@gsu.edu](mailto:agewirtz@gsu.edu)

44

45 - James D. Lewis, MD, MSCE

46 University of Pennsylvania, Center for Clinical Epidemiology and Biostatistics, 7th Floor,  
47 Blockley Hall, 423 Guardian Drive, Philadelphia, PA

48 E-Mail: [James.Lewis@pennmedicine.upenn.edu](mailto:James.Lewis@pennmedicine.upenn.edu)

49 **Abstract**

50 **Background & Aims:** Epidemiologic and murine studies suggest that dietary emulsifiers  
51 promote development of diseases associated with microbiota dysbiosis. While the detrimental  
52 impact of these compounds on the intestinal microbiota and intestinal health have been  
53 demonstrated in animal and *in vitro* models, impact of these food additives in healthy humans  
54 remains poorly characterized.

55 **Methods:** To examine this notion in humans, we performed a double-blind controlled-  
56 feeding study of the ubiquitous synthetic emulsifier carboxymethylcellulose (CMC) in which  
57 healthy adults consumed only emulsifier-free diets (n=9) or an identical diet enriched with 15  
58 grams per day of CMC (n=7) for 11 days.

59 **Results:** Relative to control subjects, CMC consumption modestly increased postprandial  
60 abdominal discomfort and perturbed gut microbiota composition in a way that reduced its  
61 diversity. Moreover, CMC-fed subjects exhibited changes in the fecal metabolome, particularly  
62 reductions in short-chain fatty acids and free amino acids. Furthermore, we identified 2 subjects  
63 consuming CMC who exhibited increased microbiota encroachment into the normally sterile inner  
64 mucus layer, a central feature of gut inflammation, as well as stark alterations in microbiota  
65 composition.

66 **Conclusions:** These results support the notion that the broad use of CMC in processed  
67 foods may be contributing to increased prevalence of an array of chronic inflammatory diseases  
68 by altering the gut microbiome and metabolome.

69

70 **Keywords:** Emulsifier, Metabolism, Microbiota, Metabolome.

## 71           **Introduction**

72           Consumption of highly processed foods has increased dramatically since the mid-20<sup>th</sup>  
73 century and is associated with increased incidence of several chronic inflammatory diseases.  
74 Among these are inflammatory bowel disease <sup>1</sup> and metabolic syndrome <sup>2</sup>, both of which are  
75 associated with, and thought to be promoted by, alterations in gut microbiota <sup>3-5</sup>. A common feature  
76 of highly processed foods is the use of one or more emulsifiers or thickeners (referred hereafter as  
77 emulsifiers), which are added to enhance texture and extend shelf-life. Some of the emulsifiers  
78 that are commonly added to foods, such as lecithin, are a natural component of unprocessed foods,  
79 while others, such as carboxymethylcellulose (CMC), are synthetic. Despite lack of extensive  
80 safety testing, CMC was approved in the 1960s for use in foods at concentrations up to 2% (wt/wt)  
81 by regulatory agencies, including the United States Food and Drug Administration and European  
82 Commission based on the GRAS (generally regarded as safe) designation developed by these  
83 agencies. Part of the basis for presuming that CMC, and some other emulsifiers, are safe is that  
84 they are not well absorbed and thus mostly eliminated in feces. However, such passage through  
85 the intestine allows these products to directly interact with gut microbiota and the intestinal  
86 mucosa. For example, CMC has been shown to impact gut transit time <sup>6</sup> and alter fecal bile acid  
87 profiles <sup>7</sup>. More recent studies show that CMC impacts human microbiota composition and gene  
88 expression *in vitro*, and in mice, wherein its impacts on gut microbiota promote the development  
89 of colitis or metabolic syndrome <sup>8-12</sup>. These findings compelled us to investigate the extent to which  
90 CMC impacts intestinal-microbiota interactions in humans.

91           Examination of how an individual food component impacts human microbiota is  
92 complicated by inter-individual heterogeneity in factors such as quantity of the food consumed,  
93 background diet quality and composition, and gut microbiota composition. To minimize the

94 potential confounding impact of these factors, we performed an in-patient (domiciled) study that  
95 assured protocol adherence, identical background diets, and enabled daily monitoring and  
96 specimen collections before, during, and after CMC consumption, or lack thereof.

Journal Pre-proof

97 **Methods**

98

99 *Study design*

100 General information: This randomized, controlled-feeding study took place in the  
101 University of Pennsylvania's Center for Human Phenomic Science (CHPS) and was registered at  
102 <https://clinicaltrials.gov> as trial no. NCT03440229. The first 3 days of the study were as an  
103 outpatient followed by 11 days as an inpatient, as presented **figure 1A**. Once admitted to the CHPS  
104 unit, participants were not allowed to leave the unit unless accompanied by study staff. The study  
105 included 16 healthy volunteers between the ages of 18 and 60 years.

106

107 Study endpoint and objectives: There were no pre-specified efficacy or safety endpoints  
108 for this study. The objectives were to 1) establish a tractable and physiologic means of measuring  
109 CMC consumption and its metabolic impact in healthy volunteers; 2) examine the extent to which  
110 CMC consumption impacts human gut microbiota composition, gene expression, and/or  
111 localization; and 3) explore effects of CMC consumption on a range of inflammatory and  
112 metabolic parameters that characterize metabolic syndrome. These included concentration of  
113 lipocalin in feces and IFN- $\gamma$ , IL-17, IL-8 and, IP-10 in serum. Additionally, insulin sensitivity was  
114 assessed with a 2.5 hour oral glucose tolerance testing performed after an overnight fast on  
115 inpatient days 1 and 11. Insulin sensitivity was measured as change in insulin divided by change  
116 in glucose from time 0 to 30 minutes.

117

118 Sample size calculation: Power calculation was based on measure of bacterial-epithelial  
119 distance, which provides a quantitative parameter whose diminution is associated with disease

120 (colitis and metabolic syndrome) in both mice and humans <sup>12, 13</sup>. Specifically, the difference in  
121 mean distance of the nearest bacteria to the epithelium between patients with and without diabetes  
122 was 19.13  $\mu\text{m}$ . The within group standard deviation (SD) for patients without diabetes was  
123 7.17  $\mu\text{m}$ . The within group SD for those with diabetes was even smaller. With a sample size of 8  
124 subjects per group and assuming a within group SD of 7.17  $\mu\text{m}$ , we projected to have 90% and  
125 80% power to detect a difference in the distance of the nearest bacteria to the epithelium between  
126 the treatment groups (CMC vs. no CMC) that is 35% and 44% smaller than the difference observed  
127 between patients with and without diabetes, respectively.

128

129 Changes to methods after trial commencement: As fully detailed **Table S1**, the study  
130 design was modified in order to improve participant recruitment. More specifically, while the first  
131 three participants stayed at CHPS for the washout period, the remaining 13 participants were  
132 allowed to go back home with provided in-house cooked food for the washout period. Moreover,  
133 while the CMC treatment duration was 14 days for the three first participants, it was 11 days for  
134 the remaining 13 participants. Importantly, the only data from days 12, 13 and 14 for the three first  
135 participants utilized in the analysis were the mucosal biopsies which were collected on day 14.

136

137 Recruitment: Participants were recruited *via* advertising the study on an online system at  
138 the University of Pennsylvania from 4/12/2018 to 1/16/2019.

139

140 Early withdrawal of participants: No participant was withdrawn from the study.

141

142            Eligibility criteria for participants: Inclusion criteria were ability to give informed consent  
143 and age 18 to 60 years. Exclusion criteria were: diagnosis with IBD, celiac disease, or other chronic  
144 intestinal disorders; baseline bowel frequency less than every 2 days or greater than 3 times daily;  
145 current smoker; body mass index (BMI) <18.5 or >40 at screening; more than two of the criteria  
146 for metabolic syndrome (waist circumference >89 cm for women or 102 cm for men, diagnosis of  
147 diabetes mellitus or baseline HbA1c > 6.4% or a fasting glucose level of greater than 100mg/dL;  
148 systolic blood pressure >130 mmHg or diastolic blood pressure >85 mmHg or treated with  
149 medications for hypertension; fasting triglycerides >149 mg/dl or treated with medications for  
150 hypertriglyceridemia; fasting HDL cholesterol <40 mg/dl in men or <50 mg/dl in women or treated  
151 with medications for hypercholesterolemia); known substance abuse disorder or consumption of  
152 illicit drugs or alcohol in the 24 hours prior to admission; prior bowel resection surgery other than  
153 appendectomy; WBC less than 3,500 per  $\mu$ L or an absolute neutrophil count of less than 1,000 per  
154  $\mu$ L; platelet count of less than 100,000 per  $\mu$ L or an INR greater than 1.2; estimated  
155 GFR<60ml/min/1.73m<sup>2</sup>; pregnant or lactating women; use of antibiotics in the 6 months prior to  
156 screening; use of laxatives or anti-diarrhea medications in the 2 weeks prior to screening; use of  
157 anticholinergic medications, narcotics, antacids, NSAIDs, or dietary supplements in the week prior  
158 to screening; HIV infection, AIDS, or other known conditions resulting in immunosuppression;  
159 allergies or intolerance to the components of the study diets; following a vegan or vegetarian diet;  
160 and experienced diarrhea within the two weeks prior to screening.

161

162            Blinding: The study employed concealed allocation with neither the participants nor the  
163 research team being aware of the treatment assignment during the screening phase and until all  
164 data were collected. The research team remained blinded to treatment assignment until all biopsies

165 had been reviewed to assess for bacteria distance from the epithelium and data were analyzed for  
166 this outcome together with the oral glucose tolerance tests and inflammatory markers.

167

168 Intervention: All food was prepared within the CHPS metabolic kitchen without  
169 emulsifiers (unless specifically added). All participants followed the same Western style diet (the  
170 only difference being portion size). The macronutrient percentages of calories for the study diet  
171 were 55% carbohydrate, 30% fat, and 15% protein. The diet provided is considered healthy with  
172 a Healthy Eating Index (HEI) score of 75<sup>14-16</sup>. The diet was composed of two menus that were  
173 consumed on alternating days. Water, black coffee, and plain tea were provided as desired.  
174 Participants had access to additional servings of food beyond the meals provided. However, the  
175 entire serving of the previous meal must have been consumed to receive additional servings.

176 For the three days prior to admission, participants ate an emulsifier free diet at home with  
177 food provided by the CHPS metabolic kitchen. After admission to CHPS, all participants  
178 consumed the same emulsifier-free diet until dinner on the first day of the inpatient stay. Thus, all  
179 participants had approximately 80 hours of emulsifier free washout time prior to administration of  
180 the food containing CMC (source: Modernist Pantry) or matched CMC-free food.

181 Participants were randomly assigned to receive 0 or 15 gm per day of CMC (9 and 7  
182 participants in each arm of the study) using concealed allocation by Dr. Hongzhe Li. Because of  
183 the small sample size, we used block randomization with a block size of 4 participants. Beginning  
184 with the dinner meal on inpatient Day 4, all participants consumed three servings of brownie and  
185 three servings of sorbet per day, each containing 0 or 2.5 gm CMC per serving. The brownie and  
186 sorbet servings were provided at three scheduled meals and three scheduled snacks. Prior to eating  
187 any other food on the study menu, participants were required to consume the brownie and sorbet

188 servings. Neither the participant nor the investigators were aware of which diet participants were  
189 assigned until the analyses of metabolic parameters, inflammatory parameters, microbiome  
190 composition and bacteria-mucosa distance assessment had been performed.

191 Physical activity was monitored during the 3-days prior to admission to CHPS through the  
192 use of a FitBit Flex. During the inpatient portion of the study, participants were required to attain  
193 within 10% of the average number of daily steps that they took in the 3 days prior to admission.

194  
195 Sample collection: Urine was collected prior to starting the outpatient study diet and each  
196 morning of the inpatient stay after an overnight fast and aliquoted and frozen at minus 80°C. Blood  
197 was collected after an overnight fast prior to breakfast at the screening visit, at a post-screening  
198 visit prior to admission, and on Days 1-4, 8, 10, and 11 of the inpatient study, and 1 month after  
199 discharge. Plasma was separated from the blood samples and stored frozen at minus 80°C for use  
200 in metabolomic studies. Stool samples were collected without preservatives or stabilizers prior to  
201 starting the outpatient diet, daily during the inpatient stay, and at 1 and 3 months after discharge.  
202 The first stool sample of the day was aliquoted and frozen at minus 80°C. All other stool samples  
203 during the inpatient stay were weighed and then discarded. On inpatient days 1 and 11 (or 14 for  
204 the first 3 participants), each participant underwent a sigmoidoscopy to obtain biopsies from the  
205 area of approximately 15 cm from the anal verge, which correlates with approximately the  
206 rectosigmoid junction. No bowel preparation was utilized prior to the sigmoidoscopy. Biopsy  
207 samples were placed in Carnoy solution for non-denaturing confocal microscopy.

208  
209 Additional data collection: We collected information on the participant's usual diet  
210 utilizing the Diet History Questionnaire II (DHQ II), a food frequency questionnaire developed by

211 the National Cancer Institute. On inpatient days 2, 3, 5, 6, 9, and 10, following lunch, participants  
212 completed a standard food satiety questionnaire utilizing a 150mm visual analog scale to measure  
213 satiety and hunger as per Doucet<sup>17, 18</sup>. Diet quality was assessed using the Healthy Eating Index  
214 2015<sup>14</sup>. On days 1 and 11, participants completed the PROMIS scales for belly pain (version 1.0  
215 – 5a) and gas/bloating (version 1.0 – 13a).

216

### 217 ***Measurements of circulating metabolic parameters and cytokines***

218 Serum cytokines were assayed using the Luminex™ 100 Multi-analyte System by  
219 University of Maryland's Cytokine Core Laboratory.

220

### 221 ***Serum lipopolysaccharide- and flagellin-specific immunoglobulins.***

222 Cf. supplemental methods section.

223

### 224 ***Microbiota analysis by 16S rRNA gene sequencing using Illumina technology***

225 Cf. supplemental methods section.

226

### 227 ***16S rRNA gene sequence analysis***

228 Cf. supplemental methods section.

229

### 230 ***Microbiota analysis by shotgun sequencing using Illumina technology***

231 Cf. supplemental methods section.

232

233

234 ***Bacterial density quantification by 16S rRNA qPCR***

235 *Cf.* supplemental methods section.

236

237 ***Quantification of fecal lipocalin-2 (Lcn-2) by ELISA***

238 For quantification of fecal Lcn-2 by ELISA, frozen fecal samples were reconstituted in  
239 PBS containing 0.1% Tween 20 to a final concentration of 100 mg/mL and vortexed for 20 min to  
240 get a homogenous fecal suspension<sup>19</sup>. These samples were then centrifuged for 10 min at 14 000  
241 g and 4°C. Clear supernatants were collected and stored at -20°C until analysis. Lcn-2 levels were  
242 estimated in the supernatants using Duoset Human Lcn-2 ELISA kit (R&D Systems, Minneapolis,  
243 MN, USA) using the colorimetric peroxidase substrate tetramethylbenzidine, and optical density  
244 (OD) was read at 450 nm (Versamax microplate reader).

245

246 ***Fecal flagellin and lipopolysaccharide load quantification***

247 *Cf.* supplemental methods section.

248

249 ***Immunostaining of mucins and localization of bacteria by FISH***

250 *Cf.* supplemental methods section.

251

252 ***Metabolomic analysis of stool and urine samples***

253 Stool and urine sample preparation for NMR were performed as previously described<sup>20</sup>.  
254 <sup>1</sup>H NMR spectra were acquired on a Bruker Avance NEO 600 MHz spectrometer equipped with  
255 an inverse cryogenic probe (Bruker Biospin, Germany) at 298 K. A typical 1D NMR spectrum  
256 named NOESYPR1D was acquired for each sample. The metabolites were assigned on the basis

257 of published results <sup>21</sup>and confirmed with a series of 2D NMR spectra. All <sup>1</sup>H NMR spectra were  
258 adjusted for phase and baseline using Chenomx (Chenomx Inc, Canada). The chemical shift of <sup>1</sup>H  
259 NMR spectra were referenced to sodium 3-trimethylsilyl [2,2,3,3-d4] propionate (TSP) at  $\delta$  0.00.  
260 **Table S2** is listing all the quantitated metabolites and their characteristics (Moieties,  $\delta$  <sup>1</sup>H (ppm)  
261 and  $\delta$  <sup>13</sup>C (ppm). The relative contents of metabolites were calculated by normalizing to the total  
262 sum of the spectral integrals. The quantification of metabolites, including CMC, in stool was  
263 calculated by NMR peak area against trimethylsilylpropanoic acid using Chenomx. The lower  
264 limit of CMC detection using the NMR approach is about >1  $\mu$ M for pure CMC and 1-10  $\mu$ M for  
265 CMC in stool and urine samples. For CMC absolute quantification, five concentrations were used  
266 in triplicates, with a lower limit of detection of 0.5 mg/ml, as presented Figure S12.

267

#### 268 *AccQ•Tag Amino Acid Analysis of Stool Samples*

269 Amino acids were extracted from stool samples with 1 mL of ice-cold methanol/water (2:1)  
270 solution (contain 2.5  $\mu$ M of Norvaline), followed by homogenization (Precellys, Bertin  
271 Technologies, Rockville, MD) with 1.0-mm-diameter zirconia/silica beads (BioSpec, Bartlesville,  
272 OK), three freeze–thaw cycles and centrifugation (Eppendorf, Hamburg, Germany). Supernatant  
273 was collected, evaporated to dryness (Thermo Scientific, Waltham, MA) and then resuspend in 50  
274  $\mu$ L 0.1N HCl solution. Amino acid derivation with AccQ•Tag reagents (Waters, Milford, MA) was  
275 conducted according to the manufacturer's protocol. Briefly, 10  $\mu$ L of stool extract were mixed  
276 with 70  $\mu$ L of AccQ•Tag Ultra borate buffer and 20  $\mu$ L of AccQ•Tag Ultra reagent in Total  
277 Recovery Vial. The vials were capped and vortex for several seconds and proceed for 10 min at  
278 55 °C. Amino Acid were detected by Waters Xevo TQS coupled with PDA, an AccQTag Ultra

279 Column (C18 1.7  $\mu\text{m}$  2.1 x 100 mm) with in-line filter (Waters, Milford, MA) were used for  
280 separation<sup>22</sup>. Results were quantified by comparing integrated peak areas against a standard curve.

281

### 282 *Statistical analysis*

283 Significance was determined using *t*-tests, Mann-Whitney test, one-way ANOVA  
284 corrected for multiple comparisons with a Bonferroni post-test, two-way ANOVA corrected for  
285 multiple comparisons with a Bonferroni post-test (or mixed-effect analysis when some values were  
286 missing), or repeated *t*-tests corrected with the false discovery rate approach where appropriate  
287 (GraphPad Prism software, version 6.01). Differences were noted as significant at  $P \leq 0.05$ .

288 **Results**

289 We enrolled 16 subjects, deemed healthy based on lack of disease history or current  
290 evidence of metabolic syndrome (see methods), who were randomly assigned with concealed  
291 allocation to the CMC-containing (n=7) or control (n=9) diets with both investigators and subjects  
292 blinded to assignments (**Figure 1A and Table S1**). The groups were similar in terms of age,  
293 gender, body mass index, and blood pressure (**Figure 1B**). At the time of screening, subjects in  
294 both groups were consuming similar diets as indicated using principal coordinate analysis (PCoA)  
295 to visualize the varied food recall responses provided by subjects upon study enrollment. (**Figure**  
296 **S1**). On study days 4-14, all subjects consumed 3 servings of brownies and 3 servings of sorbet  
297 that lacked or contained 2.5 g CMC per serving. Both groups of subjects exhibited reductions in  
298 body weight of about 1 kg and had modest improvements in glycemic control over the course of  
299 study, the extent of which did not vary significantly between the 2 groups except that a modest  
300 decrease in serum insulin levels was seen in the CMC-fed group (**Figure 1C-D**). CMC  
301 consumption was not associated with severe adverse events or alterations in serum levels of  
302 inflammatory cytokines, nor did it have an appreciable impact on appetite, food consumption, or  
303 bloating (**Figure 1E and S2**). Moreover, levels of anti-lipopolysaccharide and anti-flagellin IgG  
304 antibodies, which have been used as an indirect measure of gut permeability<sup>23,24</sup>, did not change  
305 over the course of the study in control or CMC-fed subjects (**Figure S3**). CMC consumption did  
306 associate with a modestly significant increase in postprandial abdominal pain (**Figure 1F**,  $P =$   
307 .019).

308

309

310

### 311 ***Microbiota composition***

312 Microbiota composition of daily-collected fecal specimens was characterized by 16S  
313 rRNA gene sequencing. In accord with previous studies<sup>25</sup>, PCoA of the pairwise distances  
314 (unweighted UniFrac) between samples revealed strong clustering within subjects, indicating that  
315 extent of inter-individual variations in gut microbiota composition exceeds impacts of short-term  
316 alterations in diet (**Figure 2A**, Permanova  $P = .001$ ). Consequently, as a means of focusing on the  
317 potential impact of CMC on each individual subject, we used samples collected the morning of  
318 day 4, the day on which the subjects began consuming CMC in the study, to normalize all  
319 microbiota composition data. This approach revealed that subjects fed CMC displayed greater  
320 changes in microbiota composition during the intervention period, resulting in PCoA plots  
321 showing clear treatment-based clustering after 10 days of CMC consumption (**Figure 2B**,  
322 Permanova Day 0  $P = .928$ , Day 9  $P = .228$ , Day 14  $P = .002$ ). Moreover, analysis of BrayCurtis  
323 distance changes from the morning of day 4 revealed a trend toward greater microbiota alterations  
324 during the intervention period in the CMC group compared to the control group (**Figure 2C**,  $P =$   
325  $.102$ ). These relative shifts in microbiota composition occurred without significant alterations in  
326 daily fecal weight (**Figure S4**) or fecal bacterial density between the control and CMC groups  
327 (**Figure 2D**, diet effect  $P = .503$ ). Phyla and order level analysis did not reveal significant  
328 differences in the CMC and control groups during the intervention period, (**Figure S5**).  
329 Investigation of the most significantly differentially abundant sequence variants (SVs) between  
330 CMC and control groups revealed SVs that were generally stably represented in control subjects  
331 on day 14 compared to day 4, with relative values being very close to 1 (**Figure S6**), while the  
332 relative abundance of these SVs were markedly impacted by CMC consumption, including  
333 decreases in *Faecalibacterium prausnitzii* and *Ruminococcus sp.*, and increases in *Roseburia sp.*

334 and Lachnospiraceae (**Figure S6**). While it is difficult to reliably ascribe functional consequences  
335 to these alterations, we note that CMC consumption induced loss of *F. prausnitzii*, which is  
336 associated with health and known to mediate production of beneficial metabolites such as short-  
337 chain fatty acids<sup>26-28</sup>.

338 CMC also reduced microbiota richness, which is a hallmark of various diseases states<sup>29</sup>,  
339 as revealed by decrease in the evenness (**Figure 2E**, diet effect  $P = .070$ , with  $P = .059$  at day 9  
340 and  $P = .032$  at day 14) and Shannon indices (diet effect  $P = .151$  with  $P = .091$  at day 14). To  
341 further investigate impacts of CMC on microbiota composition, we next performed shotgun  
342 metagenomic sequencing on fecal samples collected shortly before or after 10 days of CMC  
343 consumption (day 4 and 14, respectively). Quality filtered reads were assigned to taxa and  
344 function. Use of PCoA analysis of the Bray-Curtis distances to compare all of the samples (*i.e.*,  
345 pre- and post-CMC) showed within subject clustering both taxonomically and functionally  
346 (**Figures 3A and S7A**), reflecting patterns observed using 16S rRNA gene sequence data.  
347 Nonetheless, there was clear post-treatment clustering of samples from control and CMC-fed  
348 subjects based on taxonomic (**Figures S7B-C**), and, especially, function-based analysis (**Figures**  
349 **3B-C**, PCoA analysis of the Bray-Curtis distances, *cf.* method section for details). The significantly  
350 altered functional categories that drove such clustering, identified via Maaslin2, comprised a  
351 variety of microbial metabolic pathways, suggesting that CMC-induced alteration in microbiota  
352 composition might have broad impacts on microbiota function (**Fig 3D**).

353

### 354 *Changes in fecal metabolome*

355 To investigate the functional consequences of CMC's impacts on microbiota, we first  
356 measured fecal levels of molecules known to mediate host-microbiota interactions. Use of TLR4

357 and TLR5 reporter cells revealed, respectively, that fecal levels of lipopolysaccharide and flagellin  
358 were not impacted by CMC consumption (**Figure 4A, B**, mixed-effects analysis with Bonferroni  
359 multiple comparisons tests, diet effect  $P = .413$  for 4A and  $P = .220$  for 4B, Bonferroni corrected  
360  $P > .1$  for all days). There was no significant change in levels of fecal lipocalin-2, an inflammatory  
361 marker (**Figure 4C**, mixed-effects analysis with Bonferroni multiple comparisons tests, diet effect  
362  $P = .258$ , Bonferroni corrected  $P > .1$  for all days). Next, we sought to broadly examine the extent  
363 to which CMC altered the fecal metabolome, which is both shaped by gut microbiota and mediates  
364 many of its impacts on the host. We used a  $^1\text{H}$  NMR-based targeted assay capable of quantitating  
365 about 40 metabolites that are reliably detected in stools of a healthy person, many of which can be  
366 influenced by the gut microbiota. In accord with the notion that, in general, there is far less inter-  
367 person heterogeneity in microbiota metabolic function than in species composition<sup>30</sup>, we  
368 compared fecal metabolomes between control and CMC-fed subjects, without normalization to  
369 correct for basal variation amongst subjects. Accordingly, prior to CMC consumption (day 4), no  
370 significant clustering by study group was evident for the fecal metabolome (**Figure 4D**,  
371 Permanova Day 0  $P = .573$ ). In contrast, following CMC consumption, this approach showed a  
372 clear ability to distinguish fecal metabolomes of control versus CMC-fed subjects (**Figure 4D**,  
373 Permanova Day 9  $P = .001$ , Day 14  $P = .001$ ). Concomitantly, display of individual values of each  
374 metabolite for each subject on day 14 (**Figure S8**), as well as viewing mean values for each group  
375 over time *via* a heat-map (**Figure 4E**), demonstrated that fecal metabolomes of CMC-fed subjects  
376 were, on average, depleted in an array of microbiota-related metabolites, including short-chain  
377 fatty acids and essential amino acids. Such changes were clearly evident by 3 days after initiating  
378 CMC consumption and remained throughout the period of CMC consumption and had resolved  
379 when subjects were re-sampled about 1 month later (day 48) (**Figure 4E**). Moreover, NMR-based

380 detection of fecal amino acids concentration demonstrated a decrease in the fecal amounts of  
381 numerous amino acids, as presented **figure S9**. The depletion of metabolites in feces of CMC  
382 subjects occurred despite lack of significant difference in fecal bacterial density (**Figure 2D**,  
383 adjusted  $P = .503$ ) or change in total stool mass produced per subject (**Figure S4**, within group  
384 change in stool weight  $P = .903$  for control group and  $P = .990$  for CMC group), arguing against  
385 it reflecting loss of bacteria or stool dilution. Nor did CMC directly inhibit NMR-based detection  
386 of amino acids (**Figure S10**), indicating that the reductions these metabolites did not reflect a  
387 technical artifact but rather that CMC feeding depleted an array of microbiota-related metabolites.

388

### 389 *A new assay for CMC quantification*

390 Animal studies using radiolabeled CMC indicate that most of the label is eliminated in  
391 feces, suggesting that this compound is poorly absorbed<sup>31</sup>. Hence, we developed a new <sup>1</sup>H NMR-  
392 based assay which detected copious amounts of seemingly intact CMC in feces of subjects  
393 receiving the CMC-containing diet compared to participants consuming the control diet and  
394 compared to their usual diet (**Figure 4F and S11**). While the non-zero levels of CMC measured  
395 by this assay may reflect background (*i.e.*, another fecal metabolite with spectral properties similar  
396 to CMC), the significant decreased level in the participants consuming an additive-free diet ( $P <$   
397  $.05$  for all time points except day 13) and subsequent increase at day 48 and 107 after the study  
398 suggests that the readout is capturing CMC contained in processed foods that were consumed  
399 before or after participation in our study (**Figure 4G**). In further accord with the notion that CMC  
400 is not absorbed, it was undetectable in urine, nor were alterations in the urinary metabolome  
401 associated with CMC consumption (**Figure S12**). Thus, our results comport with the notion that  
402 CMC is non-absorbed but significantly altered the host-microbiota relationship.

403 *Distance between the intestinal mucosa and the microbiota and identification of CMC-sensitive*  
404 *subjects*

405 A characteristic of altered host-microbiota interactions in a range of chronic inflammatory  
406 diseases, including IBD, metabolic syndrome, and cancer, is encroachment of gut microbiota into  
407 the normally near-sterile inner mucus layer. Hence, we hypothesized that CMC consumption might  
408 result in microbiota reduce bacterial-epithelial distance as measured via confocal microscopy in  
409 distal colonic biopsies preserved in Carnoy's solution collected before or after the intervention  
410 period. On average, bacterial epithelial distance did not change over the course of the study in the  
411 control or CMC group. However, 2 individual subjects within the CMC group showed a marked  
412 reduction in this parameter, such that their biopsies showed bacteria in very close proximity to the  
413 epithelium following CMC exposure (**Figure 5A and S13**), reminiscent of observations made in  
414 patients with IBD<sup>32</sup>. Application of Fisher's Exact Test to the observation that 2 of 7 CMC-fed  
415 subjects and 0 of 9 control subjects displayed this phenotypic change over the course of the study  
416 yielded a 2-tailed  $P$  value of 0.175, which does not meet common standards of being statistically  
417 significant but nonetheless suggests a reasonable likelihood it was a consequence of CMC  
418 treatment. Accordingly, we examined if any of the clinical and/or microbiota parameters might  
419 give insight into these seemingly CMC-sensitive subjects. Although these subjects did not respond  
420 differently in terms of clinical parameters or inflammatory markers, they had significantly greater  
421 relative changes in microbiota composition in response to CMC consumption relative to other  
422 participants in the CMC group (**Figure 5B-C**, group effect  $P = .004$ ). Moreover, these subjects  
423 displayed significantly increased levels of fecal LPS (**Figure 5D**, group effect  $P = .005$ ). Analysis  
424 of the metagenomic data at the functional level using beta diversity measurement of the BrayCurtis  
425 distance revealed that these two participants had striking greater relative changes in microbiota

426 function in response to CMC consumption relative to the other participants of the CMC group  
427 (**Figure 5G**,  $P = .0002$ ). Analysis of morphometric characteristics taken at the beginning of the  
428 clinical trial revealed that CMC-sensitive subjects are both males and are older compared with  
429 other members of the CMC group, without any other significant differences (weight, height, BMI,  
430 SBP, DBP, **Figure 5H**). Collectively, these results suggest that some individuals may be prone to  
431 develop alterations in the host-microbiota interactions in response to CMC consumption, and  
432 future studies are warranted to investigate the long-term consequences on intestinal health.

433 **Discussion**

434 That the post-mid-20<sup>th</sup> century increased incidence of chronic inflammatory diseases has  
435 been roughly paralleled by increased consumption of highly processed foods has long suggested  
436 the possibility that some components of such foods promote inflammation. Appreciation of the  
437 role of the intestinal microbiota in driving inflammation led to interest in food additives capable  
438 of perturbing the host-microbiota relationship. Our previous findings that some dietary emulsifiers  
439 can impact microbiota *in vitro* and in animal models, whereby they promote inflammatory  
440 diseases, suggest that these compounds might be one specific example of this notion<sup>9-12</sup>. However,  
441 the extent to which such substances actually increase risk of disease in the doses and frequency in  
442 which they are consumed by humans remains far less clear. Our findings reported herein that  
443 consumption of one widely used food additive, namely the synthetic emulsifier  
444 carboxymethylcellulose (CMC), impacted microbiota in humans in a seemingly detrimental  
445 manner are a step toward filling this knowledge gap.

446 Epidemiologic-based studies of food additives have limited power to assess consequences  
447 of specific food additives for numerous reasons. For one, concentrations of these components in  
448 commercially prepared foods are not widely reported, making extremely challenging to  
449 quantitatively estimate food additives consumption in humans<sup>33</sup>. Furthermore, processed foods  
450 often contain multiple potentially detrimental ingredients making the driver of associations  
451 difficult to identify. Randomized control trials to assess the impact of food additives on disease  
452 incidence are very challenging due to the long period of follow-up required. Nonetheless, they  
453 remain the gold standard means to identify impact specific ingredients, for example artificial  
454 sweeteners<sup>34</sup>. Indeed, controlled feeding studies, such as ours, are ideal to study the physiologic  
455 response of humans to short-term dietary exposures in a tightly controlled setting. Our design

456 allowed us to focus on microbiota changes that are associated with chronic diseases, where a role  
457 in causation has been proposed. We observed stark changes in gut microbiota, fecal metabolome  
458 and, in a subset of the participants, encroachment of microbiota upon the gut epithelium. The  
459 predominant changes in the fecal metabolome upon CMC feeding was loss of purportedly  
460 beneficial metabolites. We envision this change likely reflected loss of key taxa and/or general  
461 disruption of microbial community homeostasis. We also demonstrate that CMC consumption can  
462 be assayed by quantitating its level in feces, thus providing a tool to facilitate longer term studies  
463 that could address extent to which CMC exposure promotes chronic diseases increasingly  
464 prevalent in developed countries.

465         The dose of CMC (15 g per person per day) used in this study likely exceeds CMC intake  
466 of most individuals but might approximate the total amount of emulsifier consumption by persons  
467 whose diets are largely comprised of highly processed foods that contain numerous emulsifiers,  
468 many of which appear to detrimentally impact human microbiotas *in vitro*<sup>8</sup>. While this study  
469 focused on one specific food additive, CMC, the results obtained support the need to apply this  
470 paradigm to other dietary emulsifiers, and mixtures thereof, at lower concentration, thus better  
471 mimicking their use in processed foods. Further, we view it as important to discern the extent to  
472 which the highly heterogenous impact of emulsifier on human microbiota *in vitro* is recapitulated  
473 *in vivo*<sup>8</sup>. Finally, while our study was not powered to discover CMC-sensitive/CMC-insensitive  
474 participants, our results nonetheless suggest that microbiota responsiveness to this food additive  
475 may be highly personalized. While follow-up studies are needed to better understand such inter-  
476 individual variability and assess its role in driving microbiota-mediated disease states, our  
477 observations argue that a particular food additive might perturb the host-microbiota relationship  
478 to promote disease in a subpopulation of individuals. If our results are confirmed in larger studies

479 with longer term follow up, the identified mechanism(s) may inform healthy food choices and  
480 enable the development of healthier processed foods.

Journal Pre-proof

481 ***Funding***

482           This work was supported by NIH grants DK115180, 5UL1TR001878 and P30-DK050306  
483 and by the Max Planck Society. BC's laboratory is supported by a Starting Grant from the  
484 European Research Council (ERC) under the European Union's Horizon 2020 research and  
485 innovation programme (grant agreement No. ERC-2018-StG- 804135), a Chaire d'Excellence  
486 from IdEx Université de Paris (ANR-18-IDEX-0001), an Innovator Award from the Kenneth  
487 Rainin Foundation, a grant from the French Research Agency (ANR-21-CE15-0042-01) and the  
488 national program "*Microbiote*" from INSERM. Funders had no role in the design of the study and  
489 data collection, analysis and interpretation, nor in manuscript writing.

490

491 ***Acknowledgment***

492           The authors thank the Penn Center for Nutritional Science and Medicine and the Human-  
493 Microbial Analytic and Repository Core of the Center for Molecular Studies in Digestive and Liver  
494 Diseases (NIH P30 DK050306). The authors thank Dr. Philip Smith from the Penn State  
495 Metabolomics Facility, and Nicholas Youngblut from the MPI. All authors had access to the study  
496 data and reviewed and approved the final manuscript.

497 **Figure legends**

498 **Figure 1: Effect of carboxymethylcellulose consumption on metabolic parameters. A.**  
499 Schematic representation of the in-patient study that enabled daily monitoring and specimen  
500 collections before, during, and after CMC consumption, or lack thereof, and presenting timing of  
501 oral glucose tolerance tests, intestinal biopsies and feces collection. **B.** Biomorphometric  
502 characterization of study's participants at the beginning of the study. **C.** Effect of dietary emulsifier  
503 CMC consumption on various metabolic parameters, measured both pre- and post- intervention.  
504 **D-F.** Effect of dietary emulsifier CMC consumption on weight (**D**), PROMISE gas/bloating (**E**)  
505 and belly pain (**F**) scores, measured both pre- and post- intervention. OGTT, Oral Glucose  
506 Tolerance Test. Significance was determined using Mann-Whitney test; \* $P < 0.05$  compared to  
507 control group.

508  
509 **Figure 2: Effect of carboxymethylcellulose consumption on microbiota composition. A.**  
510 Principal coordinates analysis of the unweighted UniFrac distance matrix of study's participants  
511 microbiota assessed by 16S rRNA gene sequencing. All time points are included in the  
512 representation, and samples are colored by participants. **B.** Principal coordinates analysis of the  
513 BrayCurtis distance matrix at days 0, 9 and 14 of study's participants microbiota composition after  
514 normalization of every SVs based on day 4 value, with samples colored by group. **C.** Changes in  
515 the microbial community structure over time, as measured by BrayCurtis distance from day 4 to  
516 subsequent days, for each group. **D.** Fecal bacterial load assessed by 16S qPCR. **E.** Changes in  
517 Evenness and Shannon alpha diversity measures for CMC intervention versus control groups, at  
518 days 0, 9 and 14. Significance was determined using two-way ANOVA corrected for multiple

519 comparisons with a Bonferroni post-test (panel **E**), multiple t-tests (panel **E**) or PERMANOVA  
520 analysis (panels **A-B**).

521

522 **Figure 3: Effect of carboxymethylcellulose consumption on fecal metagenome.** **A.** Principal  
523 coordinates analysis of the BrayCurtis dissimilarity of study's participants metagenome (uniref90  
524 categories) assessed by shotgun sequencing. Days 4 and 14 are included in the representation, and  
525 samples are colored by participants. **B-C.** Principal coordinates analysis of the BrayCurtis distance  
526 matrix at day 4 (**B**) and 14 (**C**) of study's participants metagenome assessed by shotgun  
527 sequencing, with samples colored by group.

528

529 **Figure 4: Effect of carboxymethylcellulose consumption on the fecal metabolome.** **A.** Changes  
530 of the fecal level of bioactive LPS from day 0 to subsequent days measured with HEK-TLR4  
531 reporter cells. **B.** Changes of the fecal level of bioactive flagellin from day 0 to subsequent days  
532 measured with HEK-TLR5 reporter cells. **C.** Changes of the fecal level of the inflammatory marker  
533 Lipocalin-2 from day 0 to subsequent days. **D.** Principal coordinates analysis of the Euclidean  
534 distance at days 0, 9 and 14 of study's participants' fecal metabolome, with samples colored by  
535 group. **E.** Heatmap presenting participants fecal metabolome over the course of the study. **F.**  
536 Changes of the fecal level of carboxymethylcellulose from day 0 to subsequent days in both control  
537 and CMC-treated groups. **G.** Changes of the fecal level of carboxymethylcellulose from day 0 to  
538 subsequent days in control group. Significance was determined using two-way ANOVA corrected  
539 for multiple comparisons with a Bonferroni post-test or repeated *t*-tests corrected with the false  
540 discovery rate approach for panel G; \**P* < 0.05 compared to control group for panel F, \**P* < 0.05  
541 compared to day 0 for panel G.

542

543 **Figure 5: Intersubject variability in the response to carboxymethylcellulose consumption. A.**

544 Effect of dietary emulsifier CMC consumption on microbiota localization (distance of the closest

545 bacteria from the surface of the epithelium), measured both pre- and post- intervention. **B.** Changes

546 of the BrayCurtis distance matrix, for each study's participant from the CMC-treated group, from

547 day 4 to subsequent days. **C.** Changes of the BrayCurtis distance matrix, for the CMC – Insensitive

548 and the CMC- Sensitive groups, from day 4 to subsequent days. **D.** Changes of the fecal level of

549 bioactive LPS from day 0 to subsequent days measured with HEK-TLR4 reporter cells. **E.** Changes

550 of the fecal level of bioactive flagellin from day 0 to subsequent days measured with HEK-TLR5

551 reporter cells. **F.** Changes of the fecal level of the inflammatory marker Lipocalin-2 from day 0 to

552 subsequent days. **G.** Effect of dietary emulsifier CMC consumption on fecal metagenome

553 measured through BrayCurtis distance. **H.** Biomorphometric characterization of study's

554 participants at the beginning of the study and according to CMC sensitivity status. Significance

555 was determined using one-way ANOVA corrected for multiple comparisons with a Bonferroni

556 post-test (panels A and G) or two-way ANOVA corrected for multiple comparisons with a

557 Bonferroni post-test (panels C, D, E and F). NS, not statistically significant.

558

**References**

- 559 1. Marion-Letellier R, Amamou A, Savoye G, et al. Inflammatory Bowel Diseases and Food  
560 Additives: To Add Fuel on the Flames! *Nutrients* 2019;11.
- 561 2. Martinez Steele E, Juul F, Neri D, et al. Dietary share of ultra-processed foods and  
562 metabolic syndrome in the US adult population. *Prev Med* 2019;125:40-48.
- 563 3. Caruso R, Lo BC, Nunez G. Host-microbiota interactions in inflammatory bowel disease.  
564 *Nat Rev Immunol* 2020;20:411-426.
- 565 4. Neurath MF. Host-microbiota interactions in inflammatory bowel disease. *Nat Rev*  
566 *Gastroenterol Hepatol* 2020;17:76-77.
- 567 5. Dabke K, Hendrick G, Devkota S. The gut microbiome and metabolic syndrome. *J Clin*  
568 *Invest* 2019;129:4050-4057.
- 569 6. Schultz J. Carboxymethylcellulose as a colloid laxative. *Am J Dig Dis* 1949;16:319-22.
- 570 7. Smits CH, Veldman A, Verkade HJ, et al. The inhibitory effect of carboxymethylcellulose  
571 with high viscosity on lipid absorption in broiler chickens coincides with reduced bile salt  
572 concentration and raised microbial numbers in the small intestine. *Poult Sci* 1998;77:1534-  
573 9.
- 574 8. Naimi S, Viennois E, Gewirtz AT, et al. Direct impact of commonly used dietary  
575 emulsifiers on human gut microbiota. *Microbiome* 2021.
- 576 9. Viennois E, Bretin A, Dube PE, et al. Dietary Emulsifiers Directly Impact Adherent-  
577 Invasive *E. coli* Gene Expression to Drive Chronic Intestinal Inflammation. *Cell Rep*  
578 2020;33:108229.
- 579 10. Viennois E, Merlin D, Gewirtz AT, et al. Dietary Emulsifier-Induced Low-Grade  
580 Inflammation Promotes Colon Carcinogenesis. *Cancer Res* 2017;77:27-40.
- 581 11. Chassaing B, Van de Wiele T, De Bodt J, et al. Dietary emulsifiers directly alter human  
582 microbiota composition and gene expression ex vivo potentiating intestinal inflammation.  
583 *Gut* 2017;66:1414-1427.
- 584 12. Chassaing B, Koren O, Goodrich JK, et al. Dietary emulsifiers impact the mouse gut  
585 microbiota promoting colitis and metabolic syndrome. *Nature* 2015;519:92-6.
- 586 13. Chassaing B, Raja SM, Lewis JD, et al. Colonic Microbiota Encroachment Correlates With  
587 Dysglycemia in Humans. *Cell Mol Gastroenterol Hepatol* 2017;4:205-221.
- 588 14. Krebs-Smith SM, Pannucci TE, Subar AF, et al. Update of the Healthy Eating Index: HEI-  
589 2015. *J Acad Nutr Diet* 2018;118:1591-1602.
- 590 15. Panizza CE, Shvetsov YB, Harmon BE, et al. Testing the Predictive Validity of the Healthy  
591 Eating Index-2015 in the Multiethnic Cohort: Is the Score Associated with a Reduced Risk  
592 of All-Cause and Cause-Specific Mortality? *Nutrients* 2018;10.
- 593 16. Petimar J, Smith-Warner SA, Fung TT, et al. Recommendation-based dietary indexes and  
594 risk of colorectal cancer in the Nurses' Health Study and Health Professionals Follow-up  
595 Study. *Am J Clin Nutr* 2018;108:1092-1103.
- 596 17. Doucet E, Laviolette M, Imbeault P, et al. Total peptide YY is a correlate of postprandial  
597 energy expenditure but not of appetite or energy intake in healthy women. *Metabolism*  
598 2008;57:1458-64.
- 599 18. Doucet E, Pomerleau M, Harper ME. Fasting and postprandial total ghrelin remain  
600 unchanged after short-term energy restriction. *J Clin Endocrinol Metab* 2004;89:1727-32.
- 601 19. Chassaing B, Srinivasan G, Delgado MA, et al. Fecal lipocalin 2, a sensitive and broadly  
602 dynamic non-invasive biomarker for intestinal inflammation. *PLoS One* 2012;7:e44328.

- 603 20. Jiang L, Huang J, Wang Y, et al. Eliminating the dication-induced intersample chemical-  
604 shift variations for NMR-based biofluid metabonomic analysis. *Analyst* 2012;137:4209-  
605 19.
- 606 21. Tian Y, Zhang L, Wang Y, et al. Age-related topographical metabolic signatures for the rat  
607 gastrointestinal contents. *J Proteome Res* 2012;11:1397-411.
- 608 22. Armenta JM, Cortes DF, Pisciotta JM, et al. Sensitive and rapid method for amino acid  
609 quantitation in malaria biological samples using AccQ.Tag ultra performance liquid  
610 chromatography-electrospray ionization-MS/MS with multiple reaction monitoring. *Anal*  
611 *Chem* 2010;82:548-58.
- 612 23. Cole CR, Frem JC, Schmotzer B, et al. The rate of bloodstream infection is high in infants  
613 with short bowel syndrome: relationship with small bowel bacterial overgrowth, enteral  
614 feeding, and inflammatory and immune responses. *J Pediatr* 2010;156:941-947 e1.
- 615 24. Fedirko V, Tran HQ, Gewirtz AT, et al. Exposure to bacterial products lipopolysaccharide  
616 and flagellin and hepatocellular carcinoma: a nested case-control study. *BMC Med*  
617 2017;15:72.
- 618 25. Wu GD, Chen J, Hoffmann C, et al. Linking long-term dietary patterns with gut microbial  
619 enterotypes. *Science* 2011;334:105-8.
- 620 26. Sokol H, Pigneur B, Watterlot L, et al. Faecalibacterium prausnitzii is an anti-inflammatory  
621 commensal bacterium identified by gut microbiota analysis of Crohn disease patients. *Proc*  
622 *Natl Acad Sci U S A* 2008;105:16731-6.
- 623 27. Quevrain E, Maubert MA, Michon C, et al. Identification of an anti-inflammatory protein  
624 from Faecalibacterium prausnitzii, a commensal bacterium deficient in Crohn's disease.  
625 *Gut* 2016;65:415-25.
- 626 28. Lenoir M, Martin R, Torres-Maravilla E, et al. Butyrate mediates anti-inflammatory effects  
627 of Faecalibacterium prausnitzii in intestinal epithelial cells through Dact3. *Gut Microbes*  
628 2020;12:1-16.
- 629 29. Larsen OFA, Claassen E. The mechanistic link between health and gut microbiota  
630 diversity. *Sci Rep* 2018;8:2183.
- 631 30. Human Microbiome Project C. Structure, function and diversity of the healthy human  
632 microbiome. *Nature* 2012;486:207-14.
- 633 31. Bar A, Van Ommen B, Timonen M. Metabolic disposition in rats of regular and  
634 enzymatically depolymerized sodium carboxymethylcellulose. *Food Chem Toxicol*  
635 1995;33:901-7.
- 636 32. Johansson ME, Gustafsson JK, Holmen-Larsson J, et al. Bacteria penetrate the normally  
637 impenetrable inner colon mucus layer in both murine colitis models and patients with  
638 ulcerative colitis. *Gut* 2014;63:281-91.
- 639 33. Chazelas E, Druesne-Pecollo N, Esseddik Y, et al. Exposure to food additive mixtures in  
640 106,000 French adults from the NutriNet-Sante cohort. *Sci Rep* 2021;11:19680.
- 641 34. Suez J, Korem T, Zeevi D, et al. Artificial sweeteners induce glucose intolerance by  
642 altering the gut microbiota. *Nature* 2014;514:181-6.
- 643

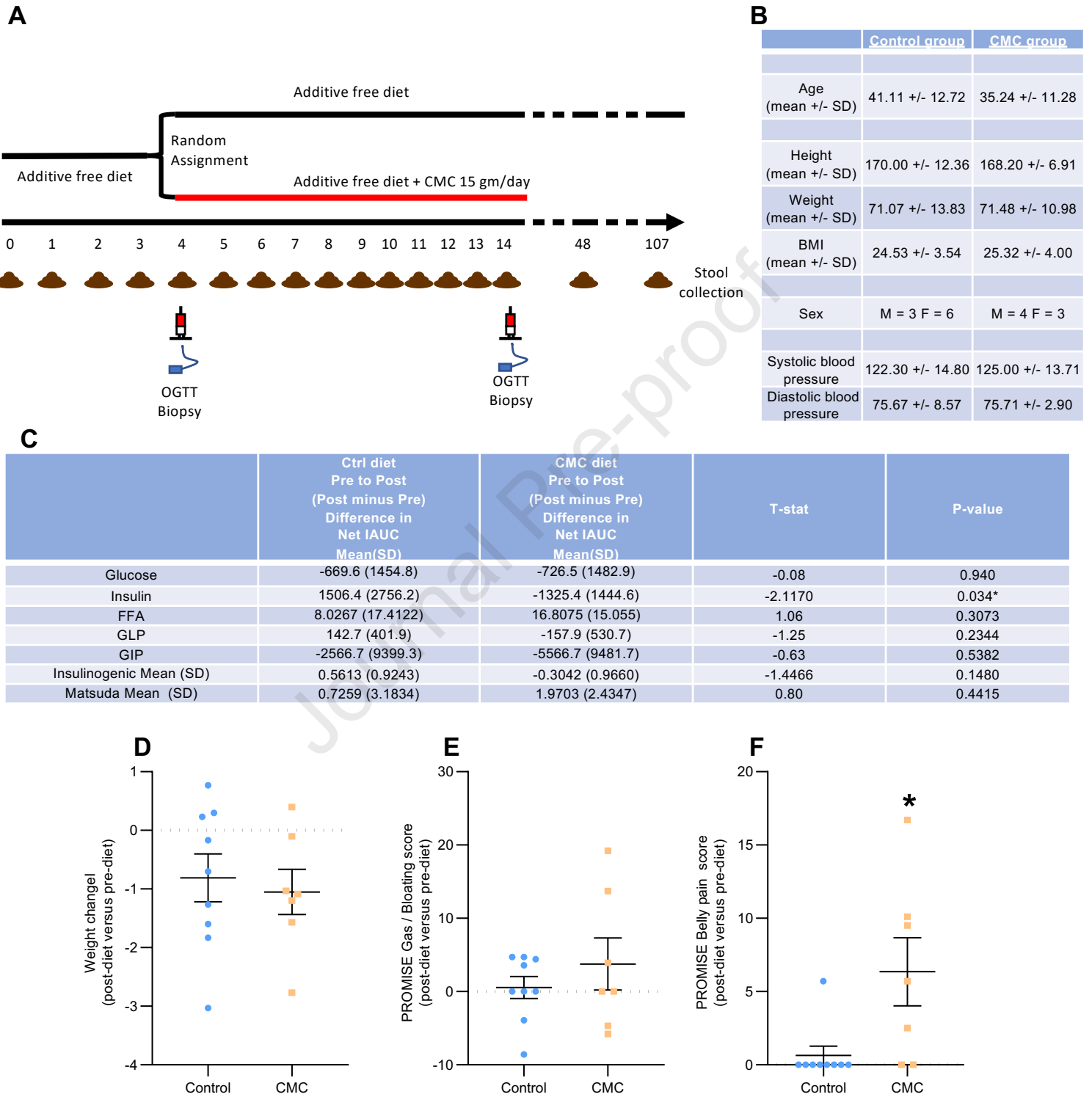


**Figure 1. Effect of carboxymethylcellulose consumption on metabolic parameters.**

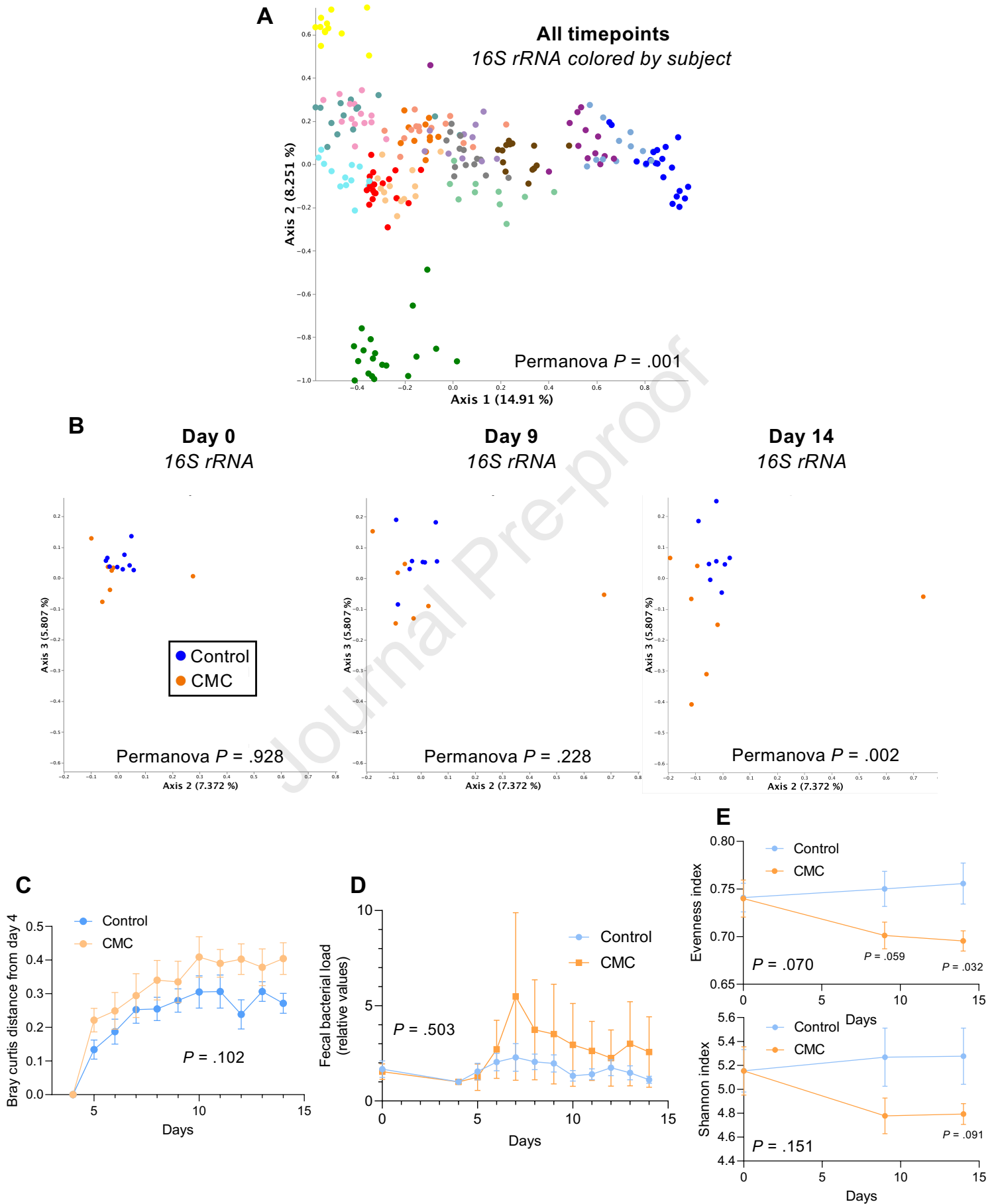


**Figure 2. Effect of carboxymethylcellulose consumption on microbiota composition.**

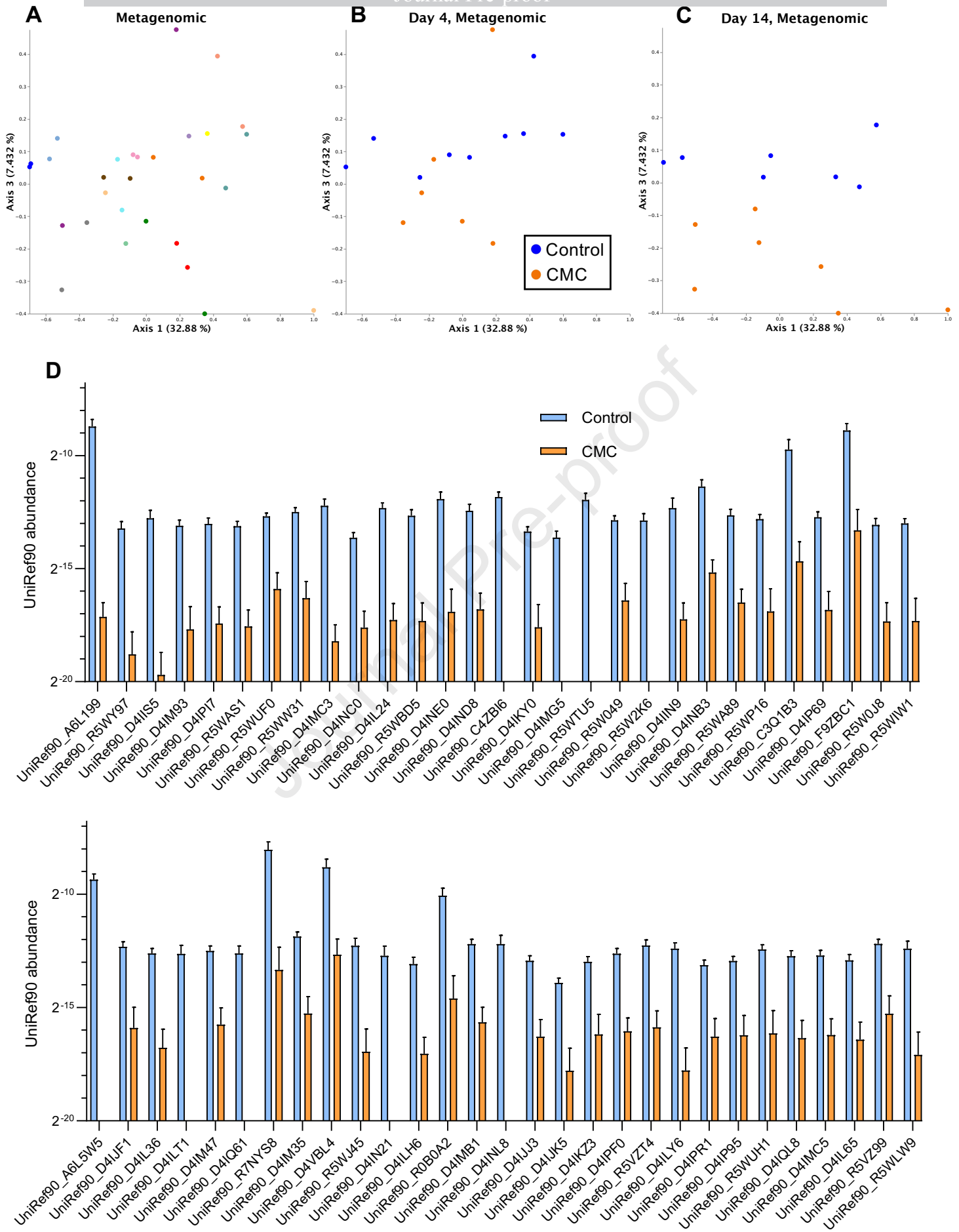


**Figure 3. Effect of carboxymethylcellulose consumption on the fecal metagenome.**

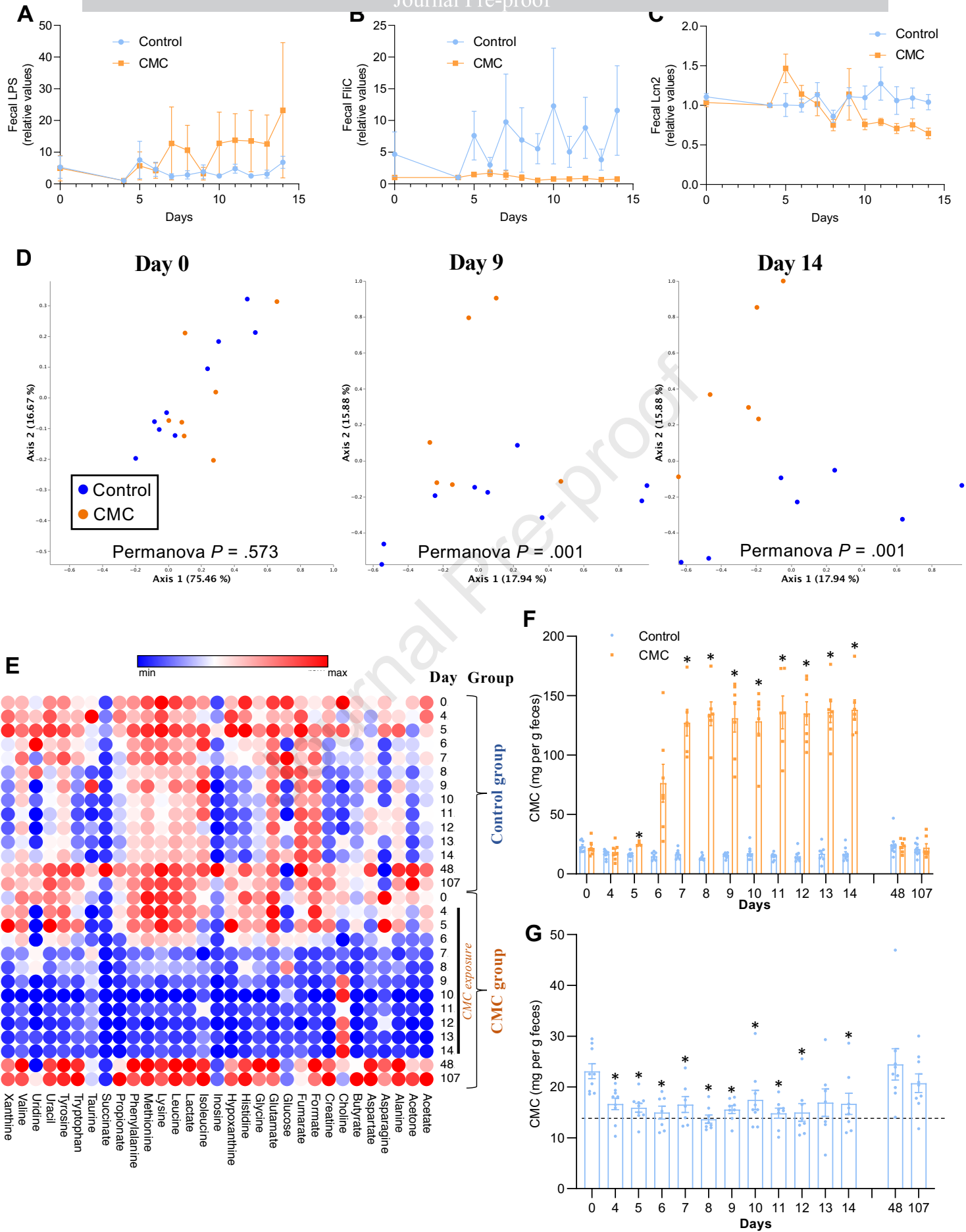


Figure 4. Effect of carboxymethylcellulose consumption on the fecal metabolome.

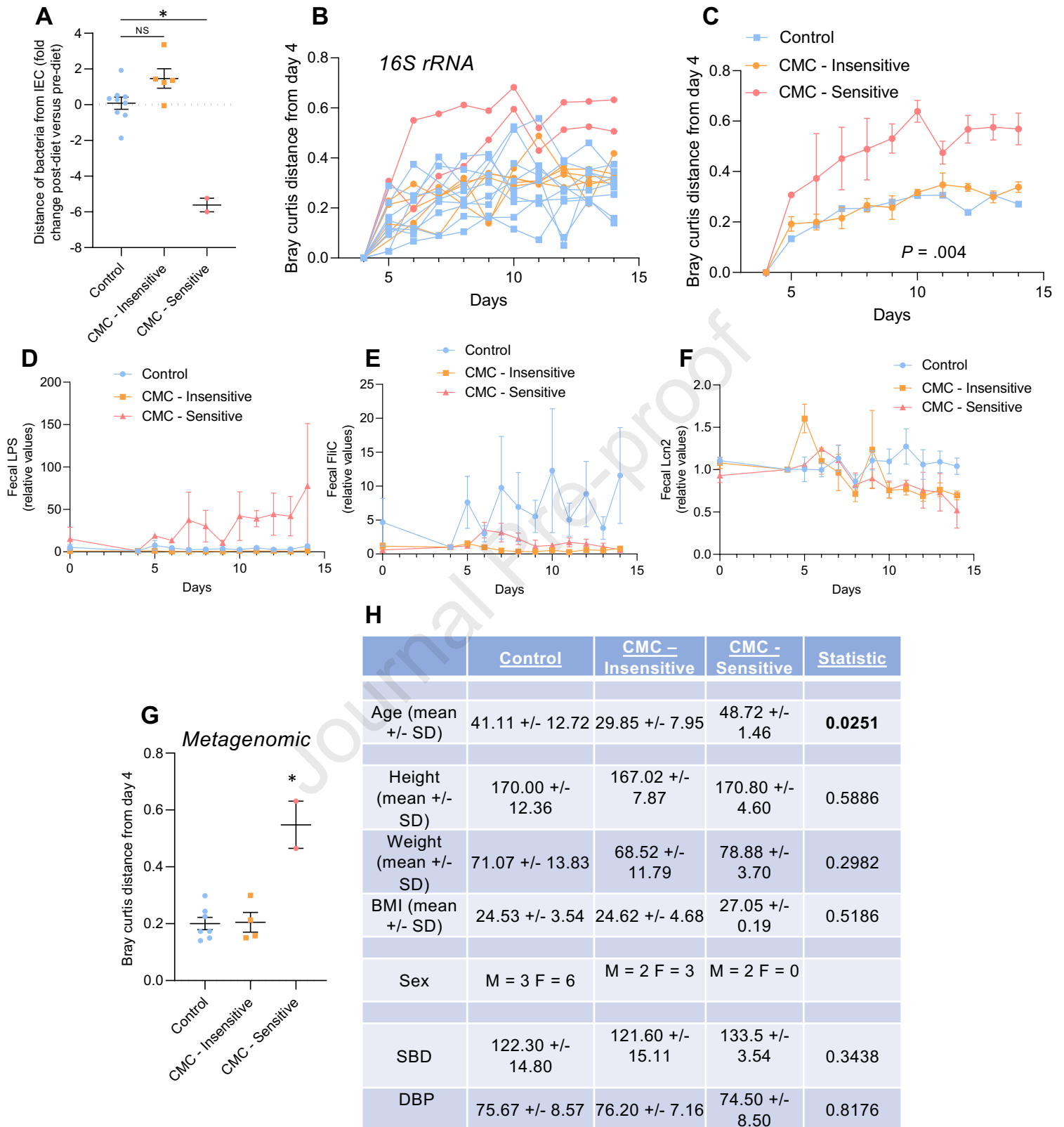
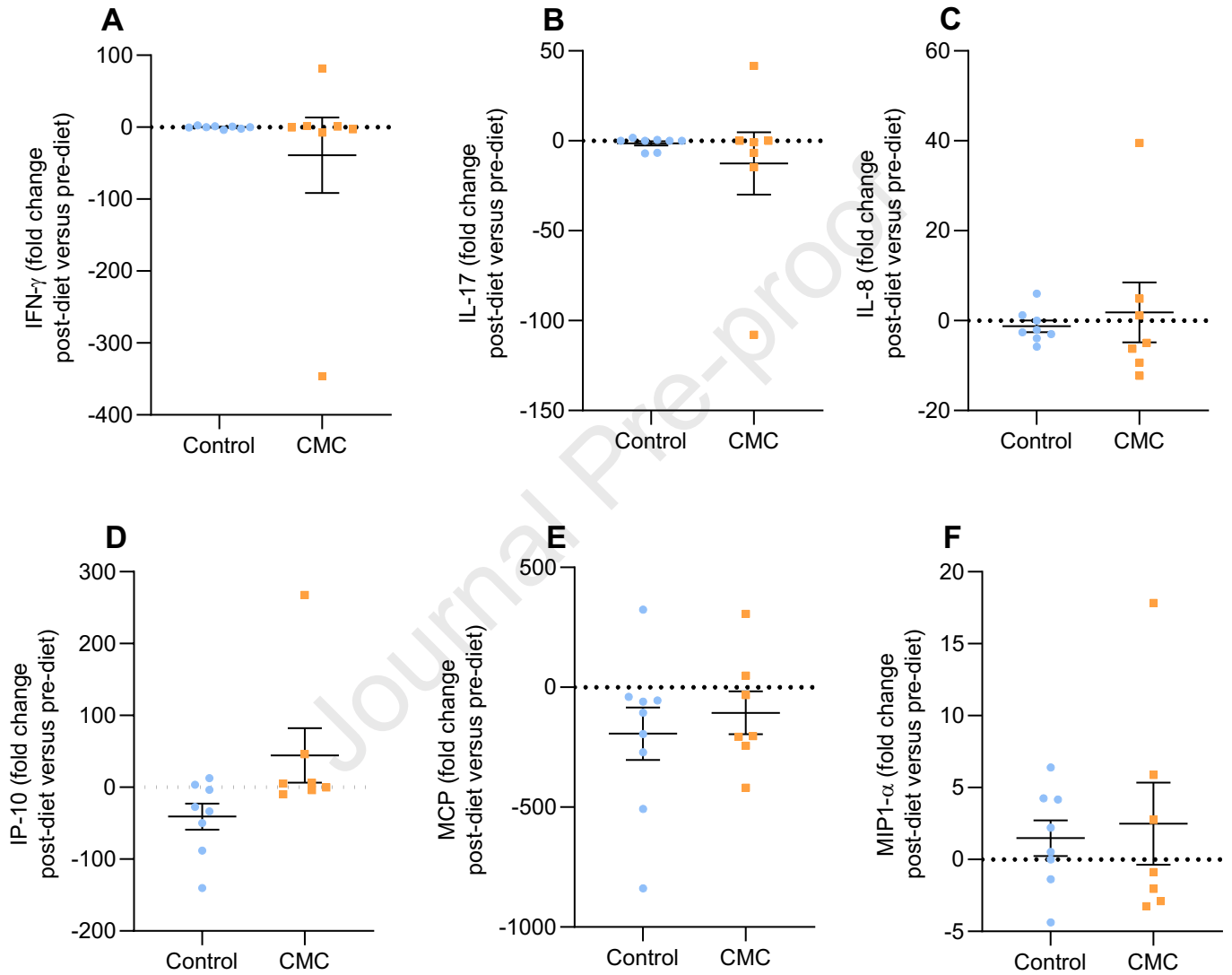


Figure 5. Intersubject variability in the response to carboxymethylcellulose consumption.

	Timepoints for the 1st three participants	Timepoints for other participants
Prior to washout period - collected at home	Day 0 - stool	Day 0 - stool
Washout period	Day 1 - stool, urine, plasma, buffy coat, serum	
Washout period	Day 2 - stool, urine, plasma, buffy coat, serum	
Washout period	Day 3 - stool, urine, plasma, buffy coat, serum	
End of washout period, last samples collected before Randomized diet phase (CMC-containing vs Emulsifier-free diet)	Day 4 - stool, urine, plasma, buffy coat, serum, OGTT, biopsies	Day 4 - stool, urine, plasma, buffy coat, serum, OGTT, biopsies
CMC exposure	Day 5 - stool, urine, plasma, buffy coat, serum	Day 5 - stool, urine, plasma, buffy coat, serum
CMC exposure	Day 6 - stool, urine	Day 6 - stool, urine, plasma, buffy coat, serum
CMC exposure	Day 7 - stool, urine	Day 7 - stool, urine, plasma, buffy coat, serum
CMC exposure	Day 8 - stool, urine, plasma, buffy coat, serum	Day 8 - stool, urine
CMC exposure	Day 9 - stool, urine	Day 9 - stool, urine
CMC exposure	Day 10 - stool, urine, plasma, buffy coat, serum	Day 10 - stool, urine
CMC exposure	Day 11 - stool, urine	Day 11 - stool, urine, plasma, buffy coat, serum
CMC exposure	Day 12 - stool, urine, plasma, buffy coat, serum	Day 12 - stool, urine
CMC exposure	Day 13 - stool, urine	Day 13 - stool, urine, plasma, buffy coat, serum
CMC exposure	Day 14 - stool, urine	Day 14 - stool, urine, plasma, buffy coat, serum, OGTT, biopsies
CMC exposure	Day 15 - stool, urine, plasma, buffy coat, serum	
CMC exposure	Day 16 - stool, urine	
CMC exposure	Day 17 - stool, urine, plasma, buffy coat, serum, OGTT, biopsies	
Post study samples	Day 48 - stool, plasma, buffy coat, serum	Day 48 - stool, plasma, buffy coat, serum
Post study samples	Day 107 - stool	Day 107 - stool

**Table S1: Timeline and list of samples collected during the study.**





**Figure S2: Impact of carboxymethylcellulose exposure on circulating cytokines.**

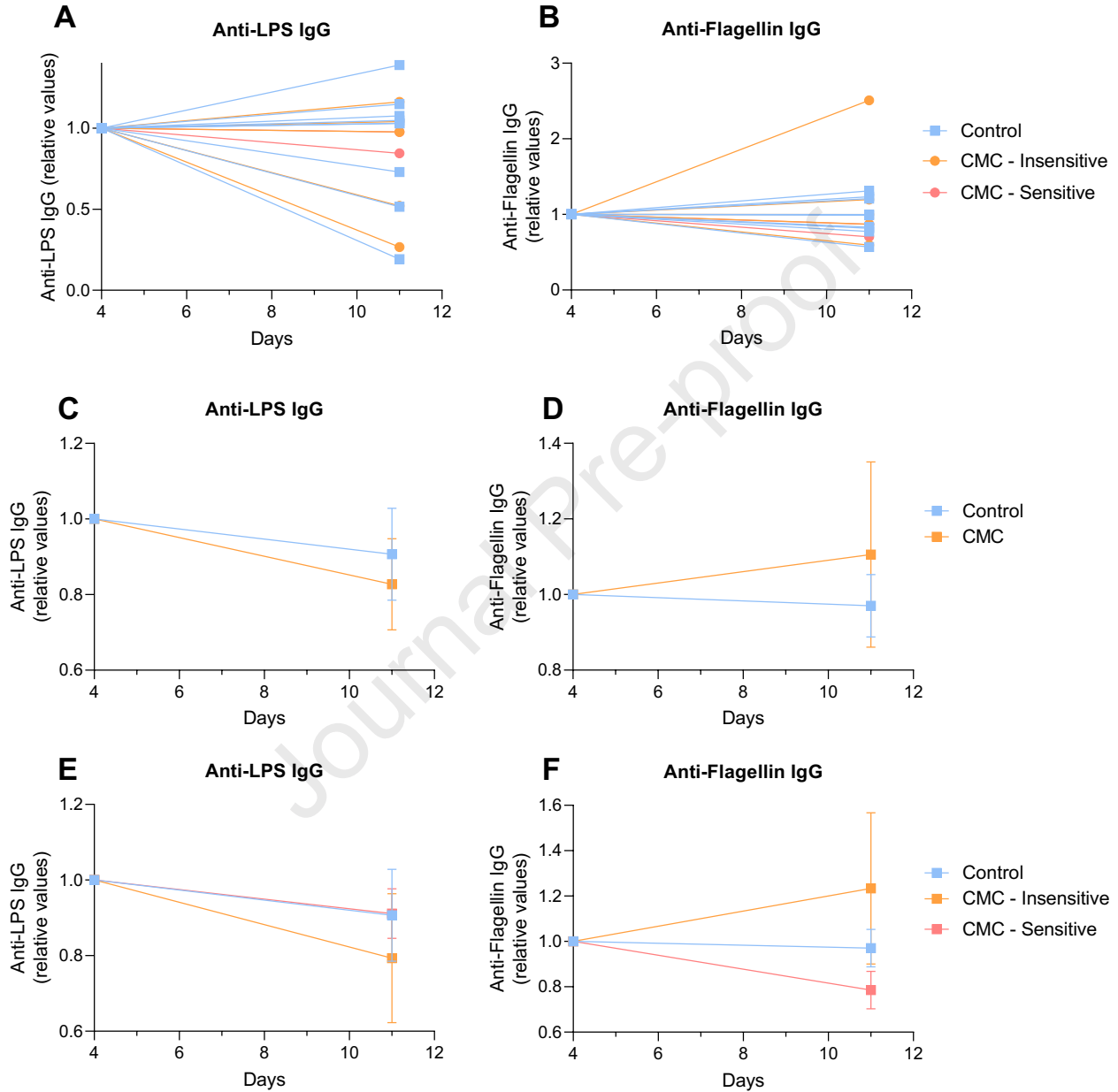


**Figure S3: Impact of carboxymethylcellulose exposure on circulating anti-lipopolysaccharide and anti-flagellin IgG.**

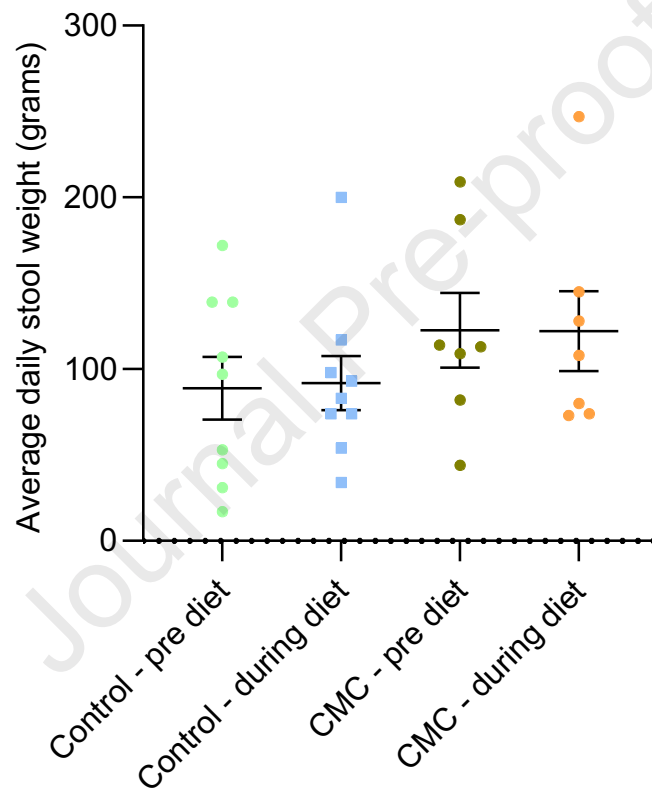


**Figure S4: Impact of carboxymethylcellulose consumption on stool weight.**

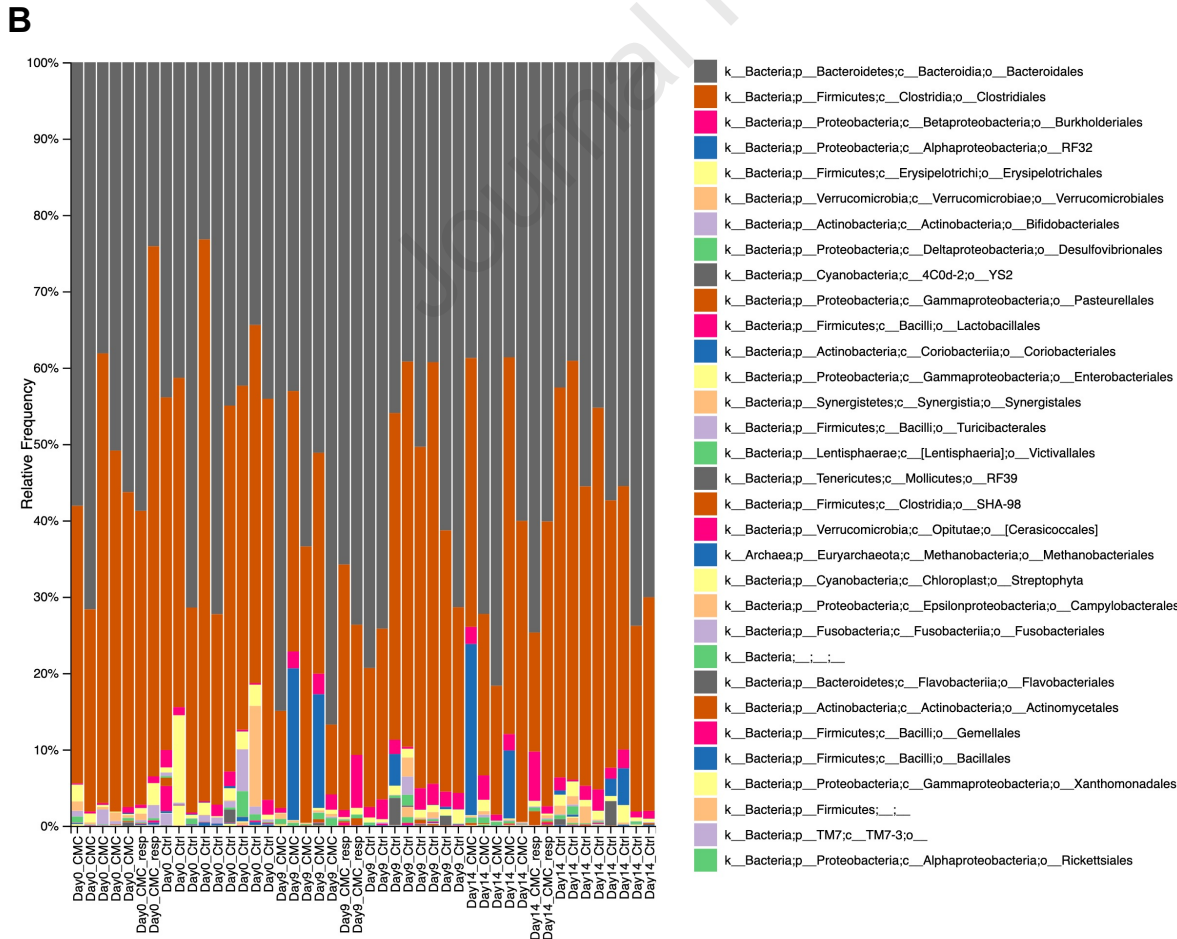
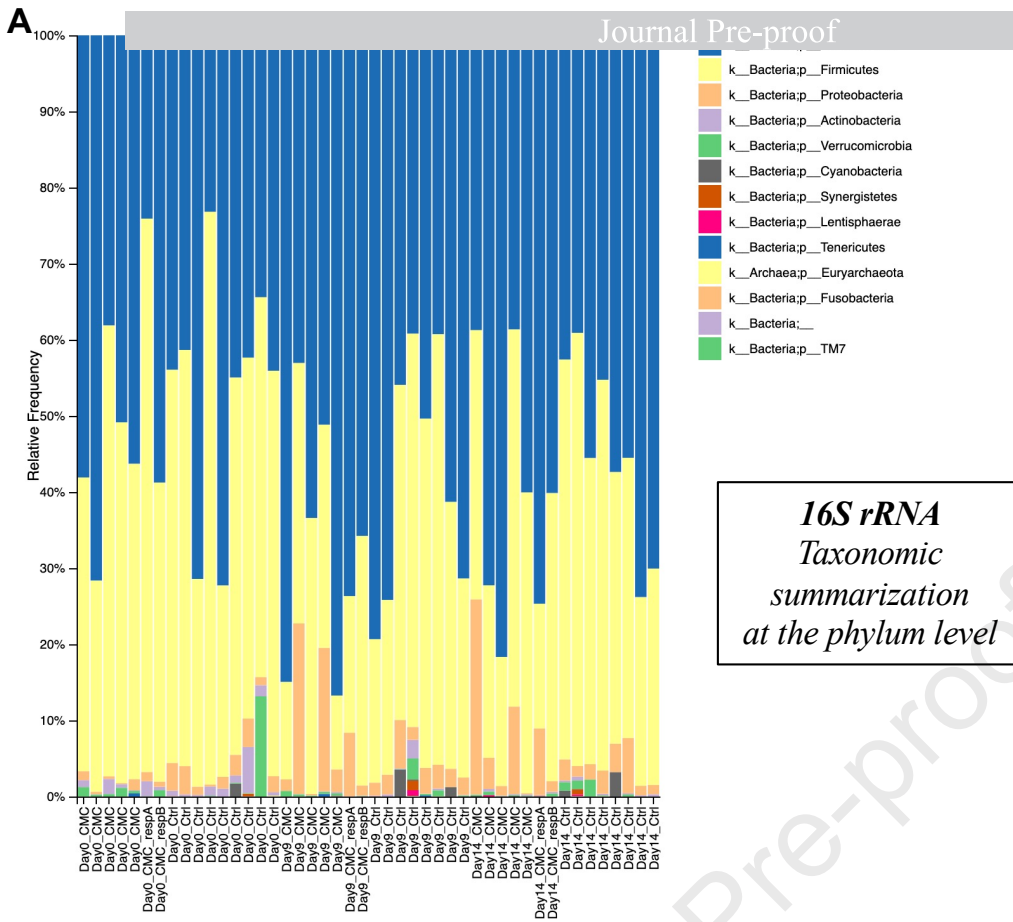


Figure S5: Effect of carboxymethylcellulose consumption on microbiota composition.

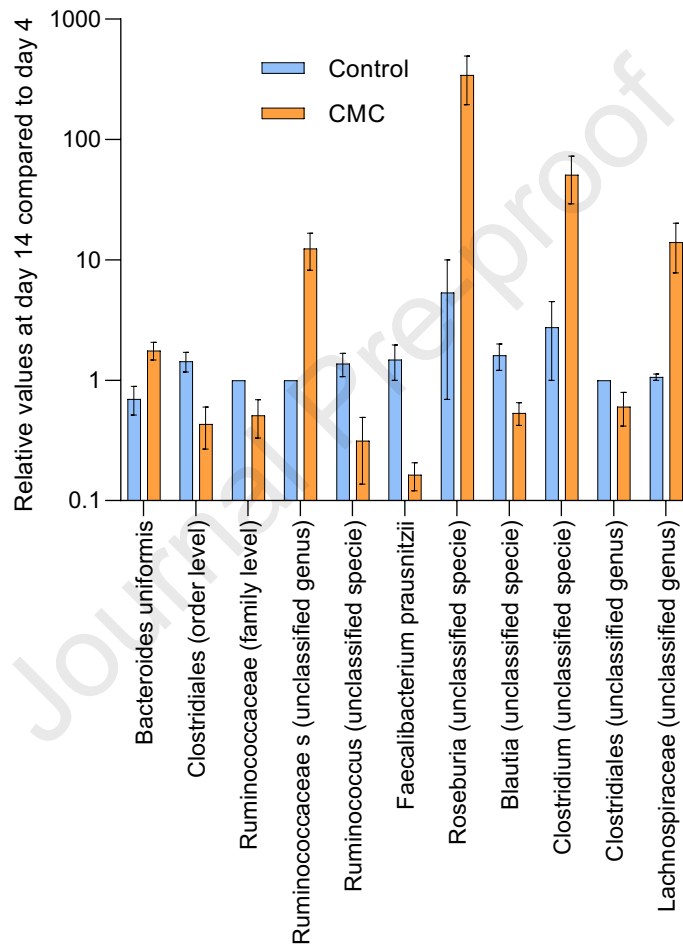
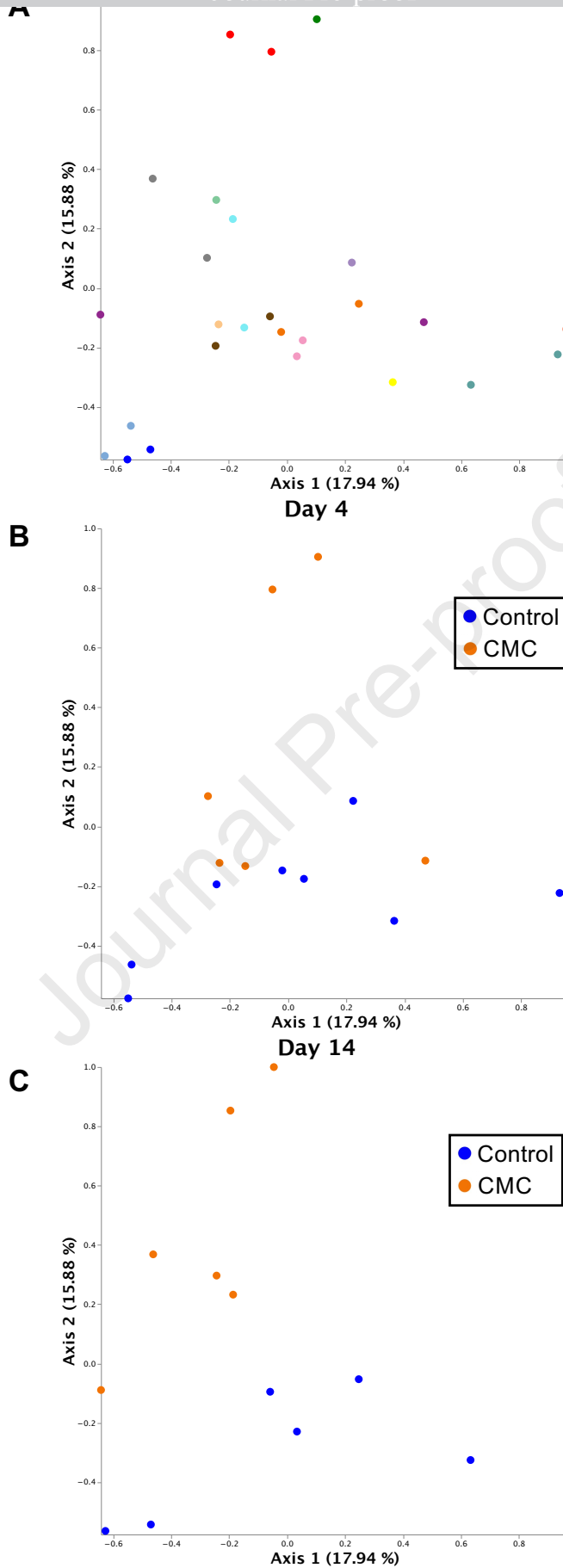


Figure S6: Effect of carboxymethylcellulose consumption on microbiota composition.



**Figure S7: Effect of carboxymethylcellulose consumption on microbiota taxonomic composition based on metagenomic data.**

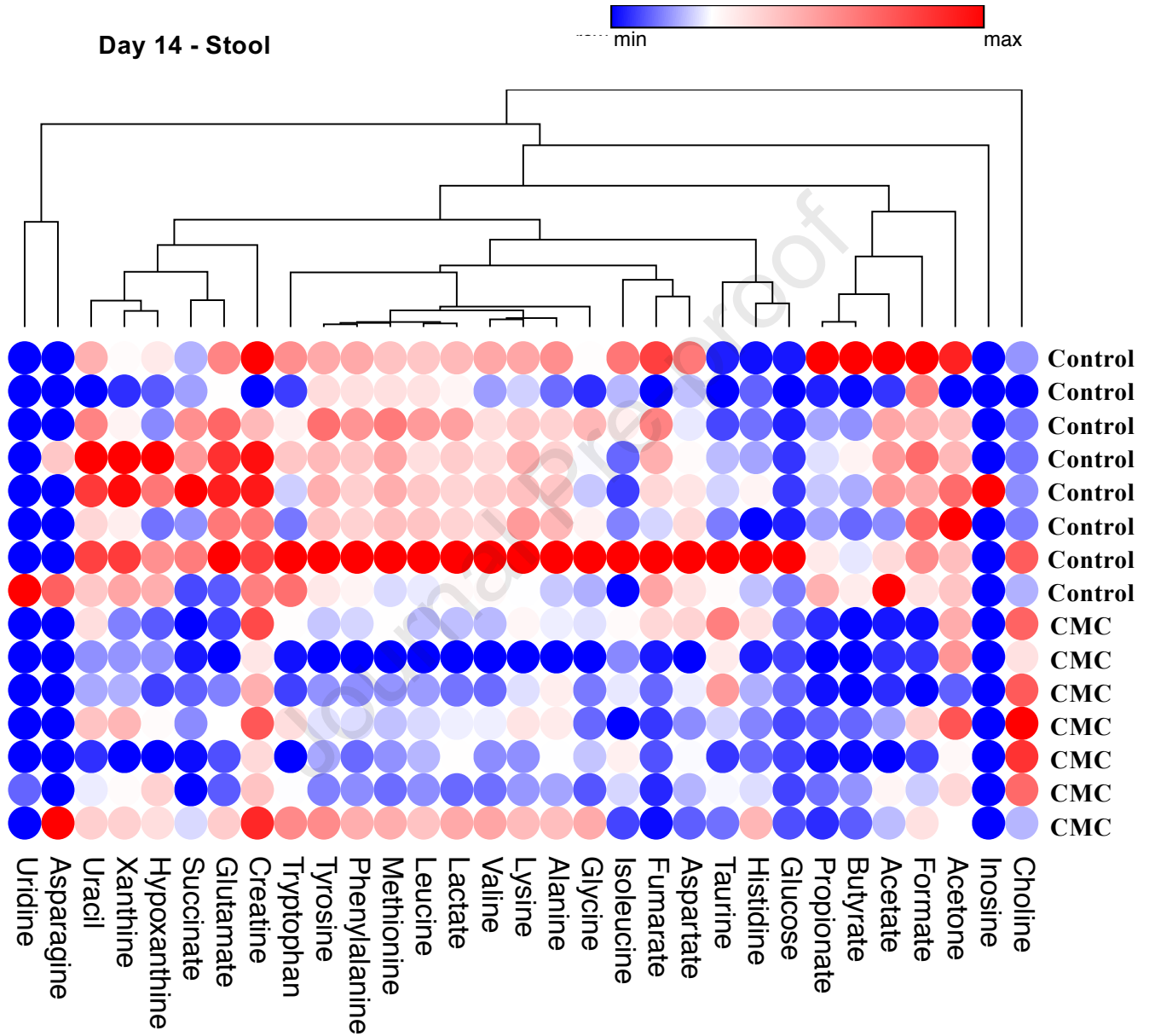
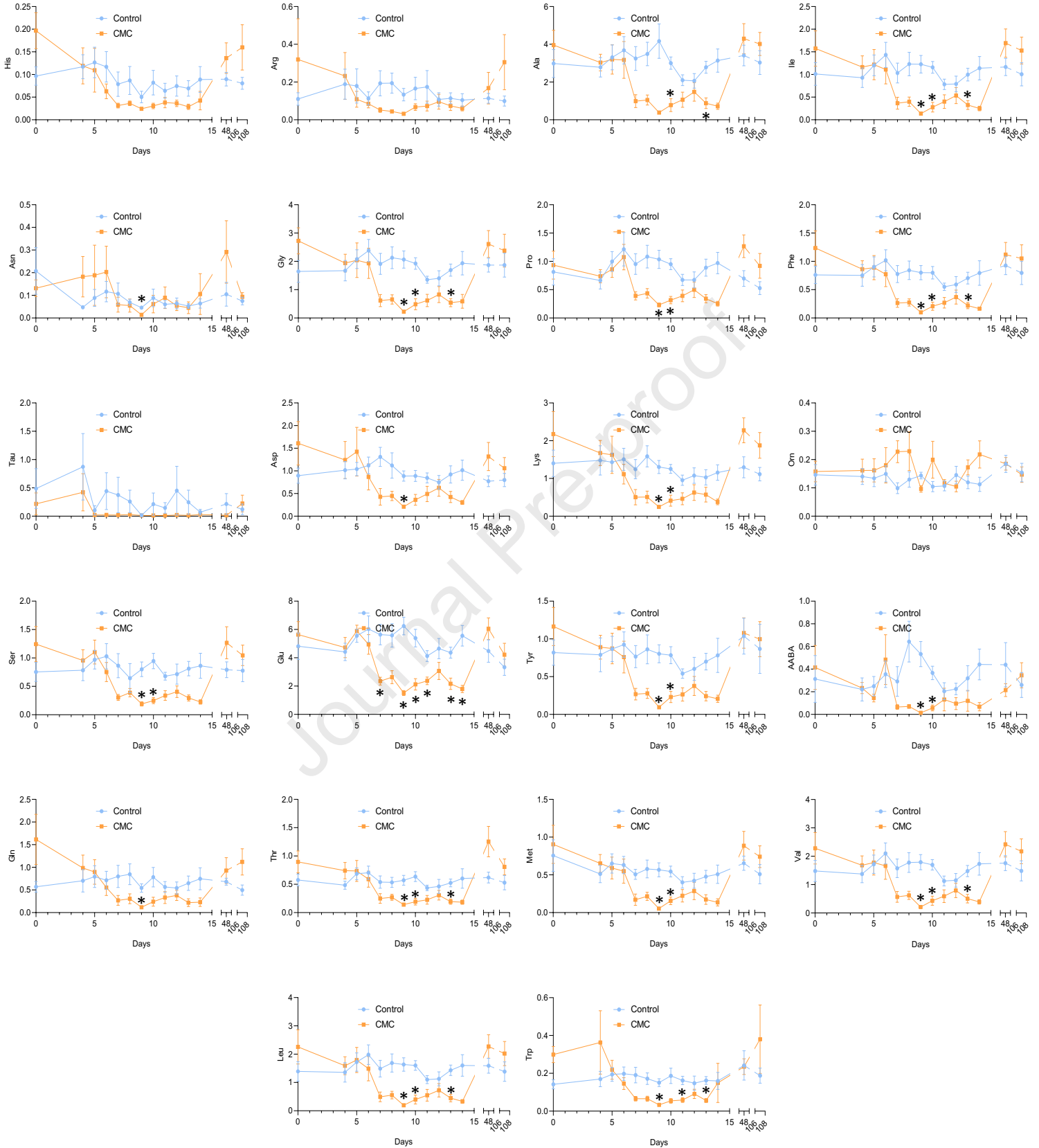
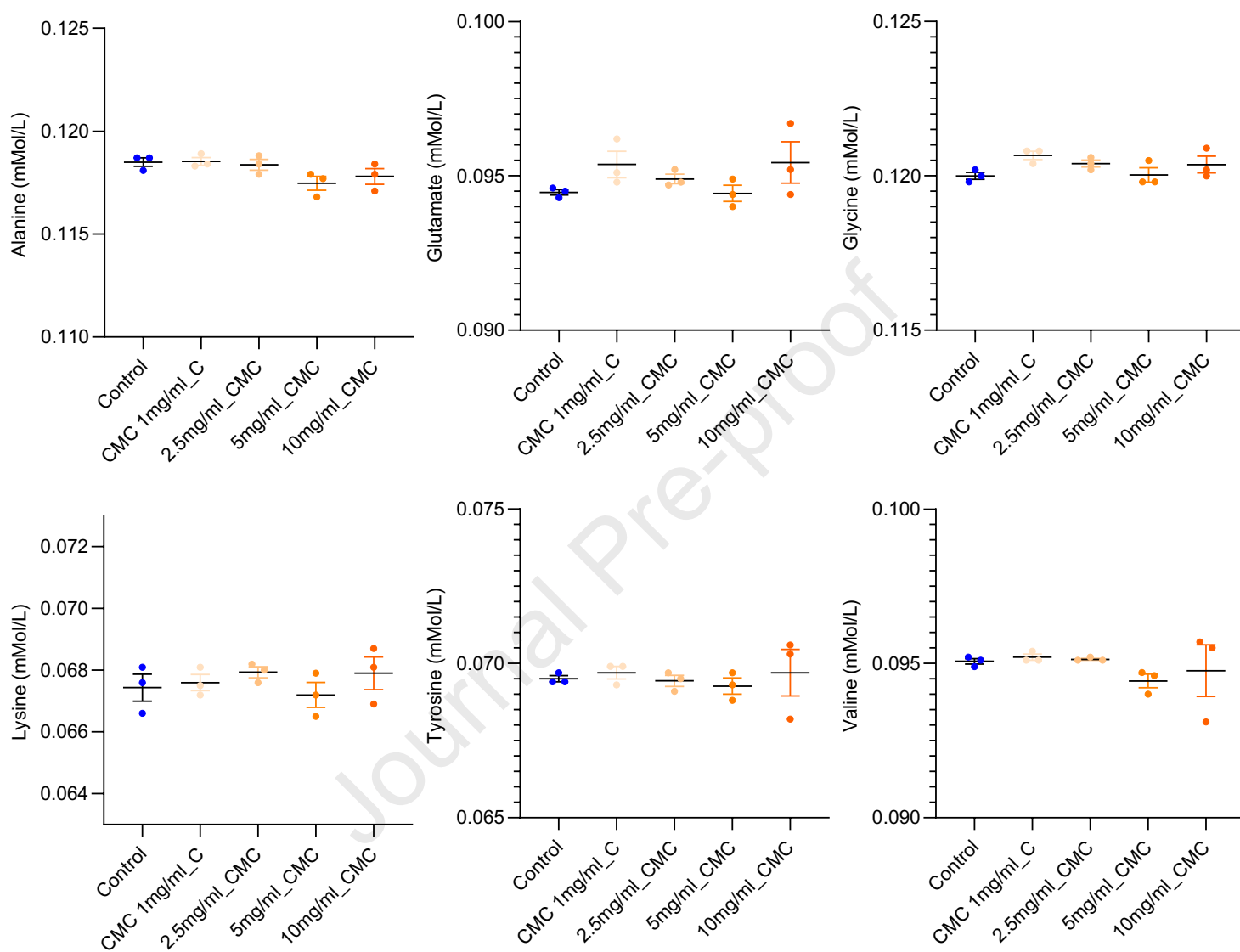


Figure S8: Effect of carboxymethylcellulose consumption on the fecal metabolome.



**Figure S9: Effect of carboxymethylcellulose consumption on the fecal metabolome**



**Figure S10: Impact of carboxymethylcellulose on AccQ•Tag-based detection of various amino acids.**

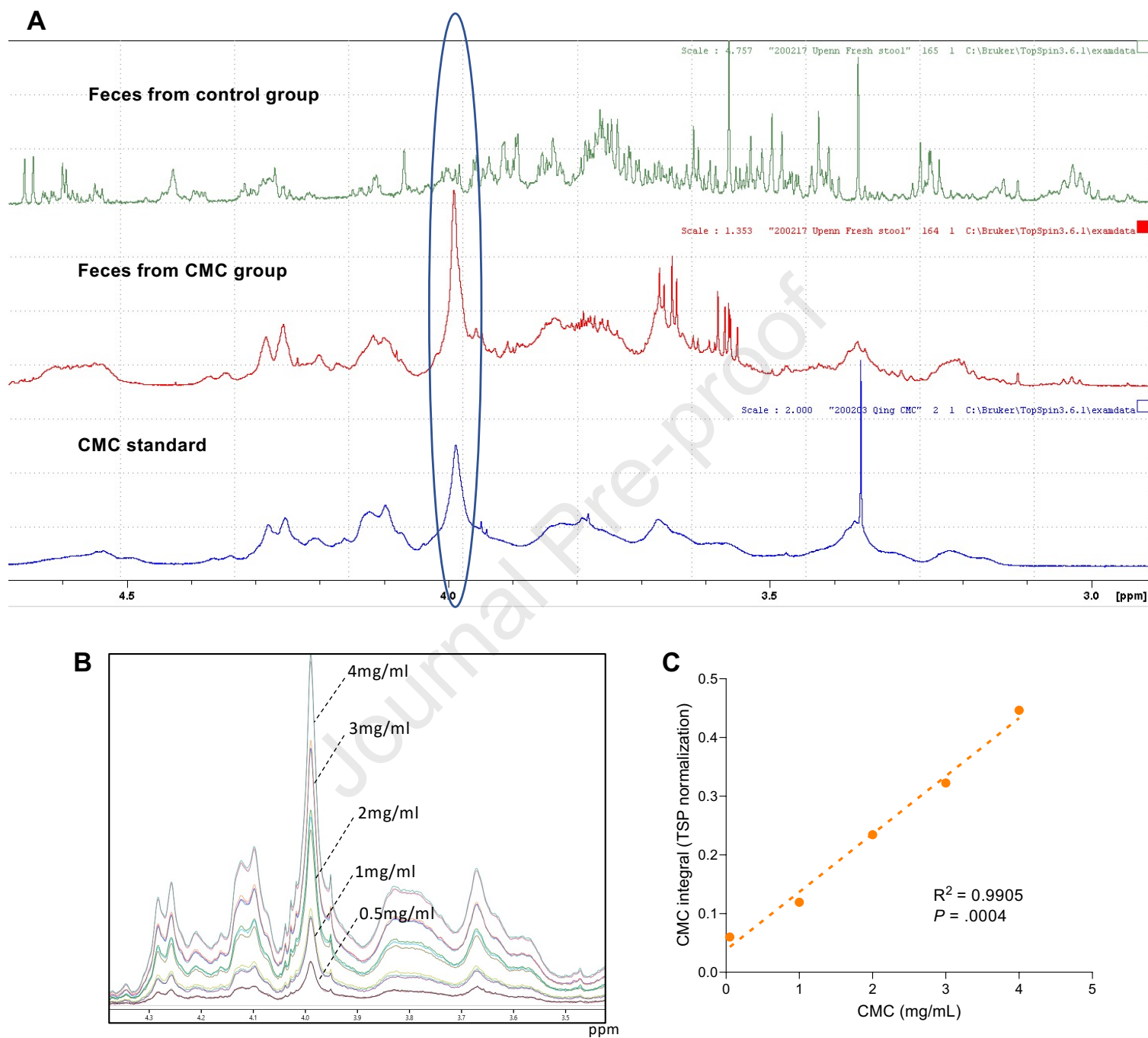


Figure S11: NMR-based detection of carboxymethylcellulose in fecal samples.

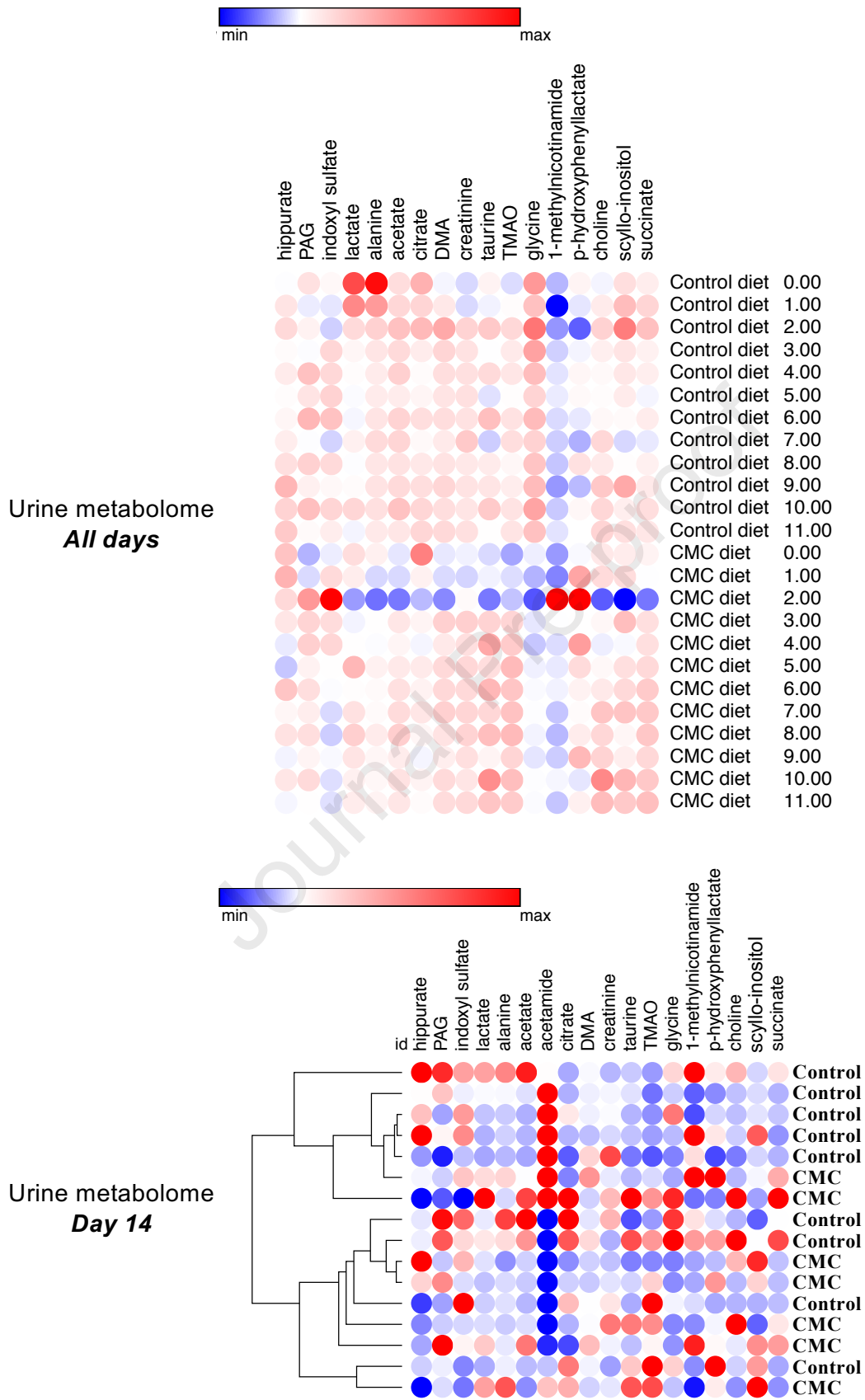
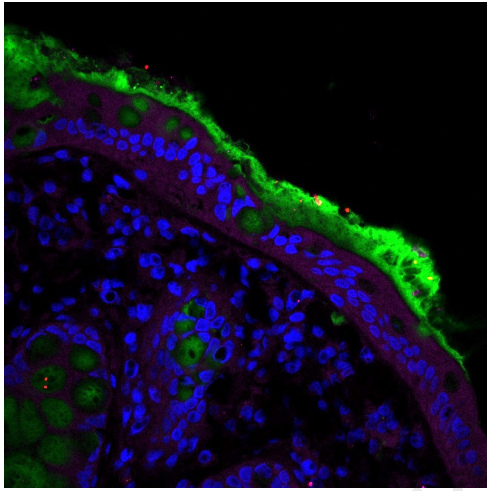
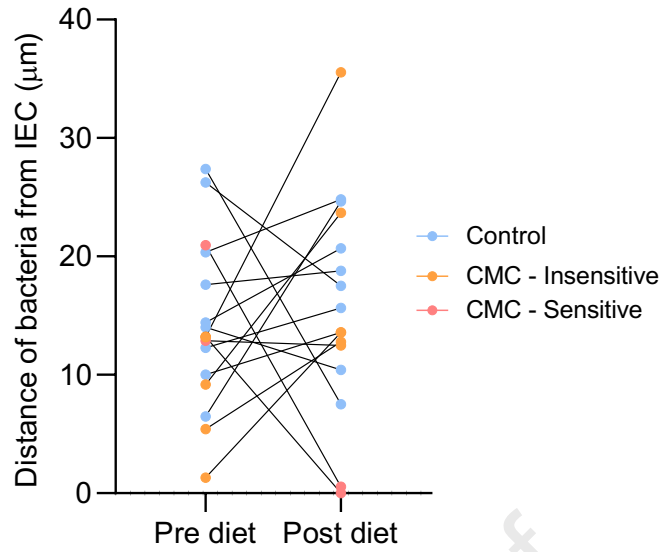
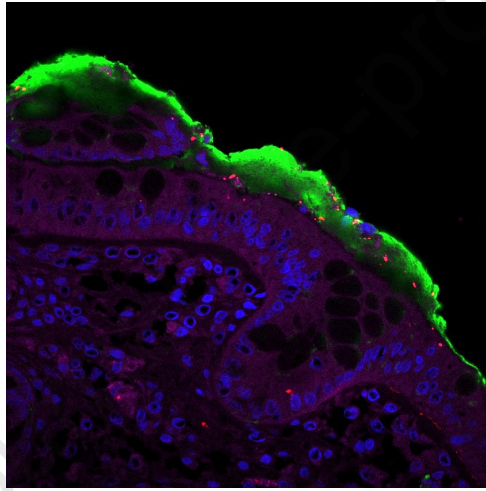


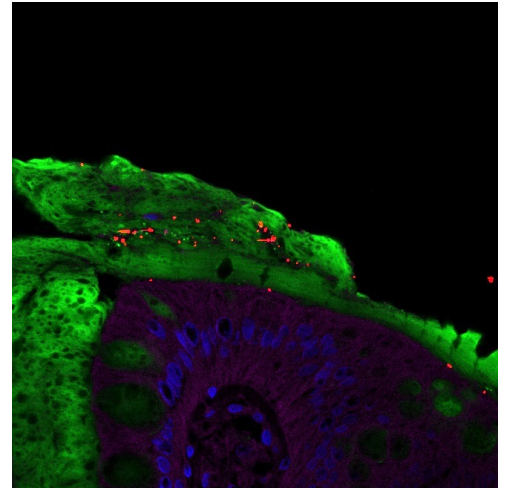
Figure S12: Effect of carboxymethylcellulose consumption on the urine metabolome.



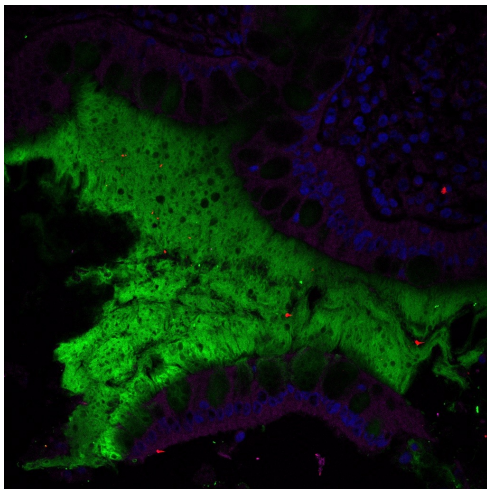
Microbiota - IEC = 14.16µm



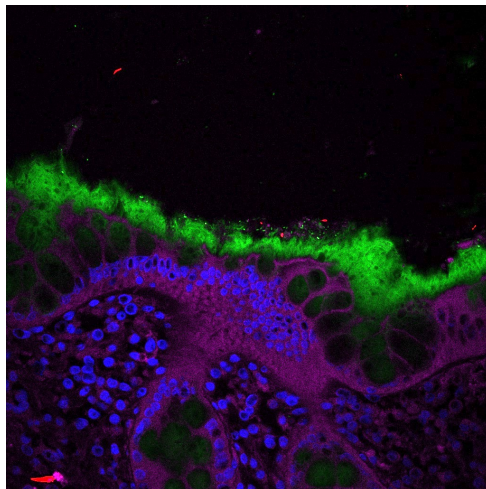
Microbiota - IEC = 2.23µm



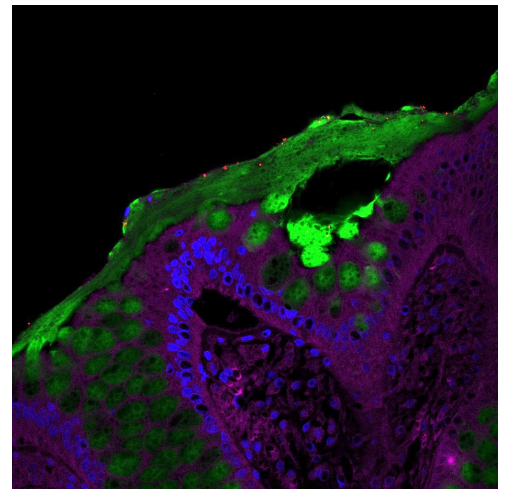
Microbiota - IEC = 0.00µm



Microbiota - IEC = 38.91µm



Microbiota - IEC = 23.86µm



Microbiota - IEC = 22.69µm

**Figure S13: Effect of carboxymethylcellulose consumption on microbiota localization**

## What You Need to Know

### BACKGROUND AND CONTEXT

Some widely used food additives, including dietary emulsifiers, alter gut microbiota and promote inflammation in *in vitro* and animal models, but applicability of such observations to humans remains poorly characterized. To begin to fill this knowledge gap, we investigated the impact of the synthetic dietary emulsifier carboxymethylcellulose (CMC) on healthy human volunteers.

### NEW FINDINGS

Addition of CMC to a healthy additive-free diet increased postprandial abdominal discomfort and altered intestinal microbiota composition. Moreover, CMC consumption starkly impacted the fecal metabolome, including depletion of health-promoting metabolites such as short-chain fatty acids and free amino acids. Furthermore, some individuals displayed microbiota encroachment into the normally sterile inner mucus layer following CMC consumption.

### LIMITATIONS

This study was focused on CMC's short-term impacts, particularly on gut microbiome. Assessing the extent to which these changes would persist in states of long-term consumption of CMC and/or other emulsifiers, and determining their phenotypic consequences, would require additional studies.

### IMPACT

That CMC consumption by humans impacted the microbiome supports the notion that wide use of this compound, and perhaps other dietary emulsifiers, in processed foods may have contributed to increased incidence of chronic inflammatory diseases.

## Lay Summary

Dietary emulsifier carboxymethylcellulose increased abdominal discomfort and altered microbiota composition and fecal metabolome, supporting the notion that its consumption may be promoting development of chronic inflammatory diseases.

## 1 Supplemental methods

2

### 3 *Serum lipopolysaccharide- and flagellin-specific immunoglobulins.*

4 Flagellin- and LPS-specific IgG levels were quantified by ELISA, as previously described  
5 <sup>1</sup>. Microtitre plates were coated overnight with purified *E. coli* flagellin (100 ng per well) or LPS  
6 (2 µg per well). Serum samples diluted 1:100 or 1:200 were then applied. After incubation and  
7 washing, wells were incubated with anti-human IgG. Quantification was performed using the  
8 colorimetric peroxidase substrate tetramethylbenzidine. Data are reported as optical density  
9 corrected by subtracting background (determined by readings in samples lacking serum) and  
10 normalized to the post-washout pre-intervention sample.

11

### 12 *Microbiota analysis by 16S rRNA gene sequencing using Illumina technology*

13 16S rRNA gene amplification and sequencing utilized the Illumina MiSeq technology  
14 following the protocol of Earth Microbiome Project with their modifications to the MOBIO  
15 PowerSoil DNA Isolation Kit procedure for extracting DNA ([www.earthmicrobiome.org/emp-](http://www.earthmicrobiome.org/emp-standard-protocols)  
16 [standard-protocols](http://www.earthmicrobiome.org/emp-standard-protocols)) <sup>2,3</sup>. Bulk DNA was extracted from frozen feces using a PowerFecal-HT kit  
17 from Qiagen with mechanical disruption (bead-beating). The 16S rRNA genes, region V4, were  
18 PCR amplified from each sample using a composite forward primer and a reverse primer  
19 containing a unique 12-base barcode, designed using the Golay error-correcting scheme, which  
20 was used to tag PCR products from respective samples <sup>3</sup>. We used the forward primer 515F 5'-  
21 *AATGATACGGCGACCACCGAGATCTACACGCTXXXXXXXXXXXXTATGGTAATTGTG*  
22 *TGYCAGCMGCCGCGGTAA*-3': the italicized sequence is the 5' Illumina adapter, the 12 X  
23 sequence is the golay barcode, the bold sequence is the primer pad, the italicized and bold sequence

24 is the primer linker and the underlined sequence is the conserved bacterial primer 515F. The  
25 reverse primer 806R used was 5'-*CAAGCAGAAGACGGCATAACGAGATAGTCAGCCAGCC*  
26 GGACTACNVGGGTWTCTAAT-3': the italicized sequence is the 3' reverse complement  
27 sequence of Illumina adapter, the bold sequence is the primer pad, the italicized and bold sequence  
28 is the primer linker and the underlined sequence is the conserved bacterial primer 806R. PCR  
29 reactions consisted of Hot Master PCR mix (Quantabio, Beverly, MA, USA), 0.2  $\mu$ M of each  
30 primer, 10-100 ng template, and reaction conditions were 3 min at 95°C, followed by 30 cycles of  
31 45 s at 95°C, 60s at 50°C and 90 s at 72°C on a Biorad thermocycler. PCRs products were  
32 quantified using Quant-iT PicoGreen dsDNA assay, a master DNA pool was generated from the  
33 purified products in equimolar ratios and subsequently purified with Ampure magnetic purification  
34 beads (Agencourt, Brea, CA, USA). The pooled product was quantified using Quant-iT PicoGreen  
35 dsDNA assay and then sequenced using an Illumina MiSeq sequencer (paired-end reads, 2 x 250  
36 bp) at Cornell University, Ithaca, NY.

37

### 38 ***16S rRNA gene sequence analysis***

39 16S rRNA sequences were analyzed using QIIME2 – version 2019 <sup>4</sup>. Sequences were  
40 demultiplexed and quality filtered using Dada2 method <sup>5</sup> with QIIME2 default parameters in order  
41 to detect and correct Illumina amplicon sequence data, and a table of Qiime 2 sequence variants  
42 (SVs) was generated. A tree was next generated, using the align-to-tree-mafft-fasttree command,  
43 for phylogenetic diversity analyses, and alpha and beta diversity analysis were computed using the  
44 core-metrics-phylogenetic command. In order to normalize for inter-individual variations in  
45 microbiota composition, day4 data were normalized at 1 for every SV identified, and the data for  
46 the other days were expressed, for each individual patient, as relative values compared to day 4

47 data. Principal coordinates analysis (PCoA) of the Unweighted Unifrac and Bray-Curtis metrics  
48 was visualized to assess the variation between experimental groups (beta diversity). For taxonomy  
49 analysis, taxonomies were assigned to SVs with a 99% threshold of pairwise identity to the  
50 Greengenes reference database 13\_8<sup>6</sup>. Unprocessed sequencing data are deposited in the European  
51 Nucleotide Archive under accession number XXXXXX.

52

### 53 ***Microbiota analysis by shotgun sequencing using Illumina technology***

54 Bulk DNA, extracted as described above for 16S rRNA gene amplicon sequencing, was  
55 processed for Illumina HiSeq sequencing in an approach similar to that described by Baym *et al.*  
56 <sup>7</sup>. Briefly, DNA concentrations were normalized, and 5ng of DNA in 10µl H<sub>2</sub>O were added to 10  
57 µl of tagmentation mix (2ul of TAPS-DMF buffer 0.25 ul Tn5 enzyme, and 7.75 ul H<sub>2</sub>O), then  
58 held for 10 min at 55°C. Next, pairwise combined Nextera indexes (N7+S5) were added to each  
59 well, followed by 25 ul of PCR reaction mix. PCR thermocycler settings were as follows: step 1  
60 72°C, 5min, step 2 98°C 30sec, step 3 98°C, 15sec, step 4 67°C, 30sec, step 5 72°C, 1min 30sec,  
61 repeat steps 3-5 13x. Samples were next pooled, and cleaned with a Zymo DNA cleanup kit.  
62 Samples were then size selected with a BluePippin on a 1.5% gel for a 350-700 base pair size  
63 range. Finally, the combined sample was diluted to 2.5nM with Illumina resuspension buffer, and  
64 sequenced on an Illumina HiSeq 3000 system at the Max Planck Institute for Developmental  
65 Biology in Tuebingen, Germany. **On average, 4.9 millions paired raw reads were obtained per  
66 samples (minimum = 2.7 millions paired raw reads, maximum = 13 millions paired raw reads).**

67 Sequencing adapters were removed from the resulting sequences *via* the bbdut module of  
68 BBDMap, version 37.78. BBDMap (align2.BBDMap) was additionally used to detect and remove  
69 human sequences<sup>8</sup>. The skewer v0.2.2 software was used to detect any remaining adapters, as well

70 as filter reads for degeneracy, and truncate and/or filter reads for low quality scores <sup>9</sup>. These  
71 quality-filtered reads were then grouped via humann2 v0.11.2 into functional categories (the  
72 chocophlan v0.1.1 nucleotide reference database, the Sep-12-2016 uniref90.ec\_filtered.1.1 protein  
73 reference file, and the Bowtie mpa\_v20\_m200 database were used as reference files for these  
74 queries) <sup>10</sup>.

75

#### 76 ***Bacterial density quantification by 16S rRNA qPCR***

77         Extracted DNAs were diluted 1/10 with sterile DNA-free water and amplified by  
78 quantitative PCR using the 16S V4 specific primers 515F 5'-GTGYCAGCMGCCGCGGTAA-3'  
79 and 806R 5'-GGACTACNVGGGTWTCTAAT-3' or using the using the AIEC LF82 PTM  
80 specific primers PTM-F 5'- CCATTCATGCAGCAGCTCTTT -3' and PTM-R 5'-  
81 ATCGGACAACATTAGCGGTGT -3' on a LightCycler 480 (Roche) using QuantiFast SYBR®  
82 Green PCR Kit (Qiagen). Amplification of a single expected PCR product was confirmed by  
83 electrophoresis on a 2% agarose gel, and data are expressed as relative values normalized with  
84 feces weight used for DNA extraction.

85

#### 86 ***Fecal flagellin and lipopolysaccharide load quantification***

87         Levels of fecal bioactive flagellin and lipopolysaccharide (LPS) were quantified as  
88 previously described <sup>11</sup> using human embryonic kidney (HEK)-Blue-mTLR5 and HEK-  
89 BluemTLR4 cells, respectively (Invivogen, San Diego, CA, USA) <sup>11</sup>. Fecal material was  
90 resuspended in PBS to a final concentration of 100 mg/mL and homogenized for 10 s using a Mini-  
91 Beadbeater-24 without the addition of beads to avoid bacteria disruption. Samples were then  
92 centrifuged at 8000 g for 2 min and the resulting supernatant was serially diluted and applied on

93 mammalian cells. Purified *E. coli* flagellin and LPS (Sigma-Aldrich) were used for standard curve  
94 determination using HEK-Blue-mTLR5 and HEK-Blue-mTLR4 cells, respectively. After 24 h of  
95 stimulation, the cell culture supernatant was applied to QUANTI-Blue medium (Invivogen) and  
96 the alkaline phosphatase activity was measured at 620 nm after 30 min.

97

### 98 ***Immunostaining of mucins and localization of bacteria by FISH***

99 Mucus immunostaining was paired with fluorescent *in situ* hybridization (FISH), as  
100 previously described<sup>12</sup>, in order to analyze bacteria localization at the surface of the intestinal  
101 mucosa<sup>13, 14</sup>. Briefly, colonic biopsies collected during rectosigmoidoscopy were placed in  
102 methanol-Carnoy's fixative solution (60% methanol, 30% chloroform, 10% glacial acetic acid) for  
103 a minimum of 3 h at room temperature, and then stored at 4°C. Tissues were then washed in  
104 methanol 2 x 30 min, ethanol 2 x 15 min, ethanol/xylene (1:1) 15 min and xylene 2 x 15 min,  
105 followed by embedding in Paraffin with a vertical orientation. Five µm sections were performed  
106 and dewax by preheating at 60°C for 10 min, followed by xylene 60°C for 10 min, xylene for 10  
107 min and 99.5% ethanol for 10 minutes. Hybridization step was performed at 50°C overnight with  
108 EUB338 probe (5'-GCTGCCTCCCGTAGGAGT-3', with a 5' labeling using Alexa 647) diluted  
109 to a final concentration of 10 µg/mL in hybridization buffer (20 mM Tris-HCl, pH 7.4, 0.9 M  
110 NaCl, 0.1% SDS, 20% formamide). After washing 10 min in wash buffer (20 mM Tris-HCl, pH  
111 7.4, 0.9 M NaCl) and 3 x 10 min in PBS, PAP pen (Sigma-Aldrich) was used to mark around the  
112 section and block solution (5% fetal bovine serum in PBS) was added for 30 min at 4°C. Mucin-2  
113 primary antibody (rabbit H-300, Santa Cruz Biotechnology, Dallas, TX, USA) was diluted 1:1500  
114 in block solution and apply overnight at 4°C. After washing 3 x 10 min in PBS, block solution  
115 containing anti-rabbit Alexa 488 secondary antibody diluted 1:1500, Phalloidin-

116 Tetramethylrhodamine B isothiocyanate (Sigma-Aldrich) at 1 $\mu$ g/mL and Hoechst 33258 (Sigma-  
117 Aldrich) at 10 $\mu$ g/mL was applied to the section for 2h. After washing 3 x 10 min in PBS slides  
118 were mounted using Prolong anti-fade mounting media (Life Technologies, Carlsbad, CA, USA).  
119 Observations were performed with a Zeiss LSM 700 confocal microscope with software Zen 2011  
120 version 7.1. This software was used to determine the distance between bacteria and epithelial cell  
121 monolayer, as well as the mucus thickness.

122

### 123 *Metabolomic analysis of stool and urine samples*

124 Stool and urine sample preparation for NMR were performed as previously described<sup>15</sup>.  
125 <sup>1</sup>H NMR spectra were acquired on a Bruker Avance NEO 600 MHz spectrometer equipped with  
126 an inverse cryogenic probe (Bruker Biospin, Germany) at 298 K. A typical 1D NMR spectrum  
127 named NOESYPR1D was acquired for each sample. The metabolites were assigned on the basis  
128 of published results<sup>16</sup> and confirmed with a series of 2D NMR spectra. All <sup>1</sup>H NMR spectra were  
129 adjusted for phase and baseline using Chenomx (Chenomx Inc, Canada). The chemical shift of <sup>1</sup>H  
130 NMR spectra were referenced to sodium 3-trimethylsilyl [2,2,3,3-d<sub>4</sub>] propionate (TSP) at  $\delta$  0.00.  
131 The relative contents of metabolites were calculated by normalizing to the total sum of the spectral  
132 integrals. The quantification of metabolites including CMC in stool was calculated by NMR peak  
133 area against TSP using Chenomx.

134

### 135 *AccQ•Tag Amino Acid Analysis of Stool Samples*

136 Amino acids were extracted from stool samples with 1 mL of ice-cold methanol/water (2:1)  
137 solution (contain 2.5  $\mu$ M of Norvaline), followed by homogenization (Precellys, Bertin  
138 Technologies, Rockville, MD) with 1.0-mm-diameter zirconia/silica beads (BioSpec, Bartlesville,

139 OK), three freeze–thaw cycles and centrifugation (Eppendorf, Hamburg, Germany). Supernatant  
140 was collected, evaporated to dryness (Thermo Scientific, Waltham, MA) and then resuspend in 50  
141  $\mu\text{L}$  0.1N HCl solution. Amino acid derivation with AccQ•Tag reagents (Waters, Milford, MA) was  
142 conducted according to the manufacturer’s protocol. Briefly, 10  $\mu\text{L}$  of stool extract were mixed  
143 with 70  $\mu\text{L}$  of AccQ•Tag Ultra borate buffer and 20  $\mu\text{L}$  of AccQ•Tag Ultra reagent in Total  
144 Recovery Vial. The vials were capped and vortex for several seconds and proceed for 10 min at  
145 55 °C. Amino Acid were detected by Waters Xevo TQS coupled with PDA, an AccQTag Ultra  
146 Column (C18 1.7  $\mu\text{m}$  2.1 x 100 mm) with in-line filter (Waters, Milford, MA) were used for  
147 separation <sup>17</sup>. Results were quantified by comparing integrated peak areas against a standard curve.

148

#### 149 *Statistical analysis*

150 Significance was determined using *t*-tests, Mann-Whitney test, one-way ANOVA  
151 corrected for multiple comparisons with a Bonferroni post-test, two-way ANOVA corrected for  
152 multiple comparisons with a Bonferroni post-test (or mixed-effect analysis when some values were  
153 missing), or repeated *t*-tests corrected with the false discovery rate approach were appropriate  
154 (GraphPad Prism software, version 6.01). Differences were noted as significant at  $P \leq 0.05$ .

155 **Supplementary figure legends**

156

157 **Table S1: Timeline and list of samples collected during the study.**

158

159 **Table S2: NMR data for the metabolites found in stool (S) and urine (U).**

160

161 **Figure S1: Dietary habits did not significantly differ between groups at the beginning of the**  
162 **study.** Principal coordinates analysis of the Euclidean distance matrix based on the Dietary History  
163 Questionnaire II, a semi-quantitative food frequency questionnaire developed by the NCI. Samples  
164 are colored by group.

165

166 **Figure S2: Impact of CMC exposure on circulating cytokines. A-F.** Effect of dietary emulsifier  
167 CMC consumption on circulating IFN- $\gamma$  (A), IL-17 (B), IL-8 (C), IP-10 (D), MCP-1 (E) and MIP-  
168 1 $\alpha$  (F) scores, measured both pre- and post- intervention. Significance was determined using *t*-  
169 test. IFN, Interferon; IL, Interleukin; IP, Inducible protein; MCP, Monocyte Chemoattractant  
170 Protein ; MIP, Macrophage inflammatory protein.

171

172 **Figure S3: Impact of CMC exposure on circulating anti-lipopolysaccharide and anti-flagellin**  
173 **IgG.** Effect of dietary emulsifier CMC consumption on circulating anti-lipopolysaccharide (A, C,  
174 E) and anti-flagellin (B, D, F) IgG levels, measured both pre- and post- intervention with data  
175 normalized to 1 for the pre-intervention value. In A and B, individual participants are represented.  
176 In C, D, E and F values are averaged by group.

177

178 **Figure S4: Impact of carboxymethylcellulose consumption on stool weight.** Daily stool weight  
179 production of study's participants measured before and during the study.

180

181 **Figure S5: Effect of carboxymethylcellulose consumption on microbiota composition.**  
182 Microbiota composition of study's participants at days 0, 9 and 14 at the phylum (A) and order (B)  
183 levels.

184

185 **Figure S6: Effect of carboxymethylcellulose consumption on microbiota composition.** List of  
186 the most significantly altered microbiota members between control and CMC-treated study's  
187 participants after normalization of every SVs based on day 4 value. These microbiota members  
188 were the most significant between groups when using repeated *t*-tests corrected with a false  
189 discovery rate approach (q-values < .05).

190

191 **Figure S7: Effect of carboxymethylcellulose consumption on microbiota taxonomic  
192 composition based on metagenomic data.** A. Principal coordinates analysis of the BrayCurtis  
193 dissimilarities of study's participants microbiota metagenome assessed by shotgun sequencing. All  
194 time points are included in the representation, and samples are colored by participants. B. Principal  
195 coordinates analysis of the BrayCurtis dissimilarities of study's participants day 4 microbiota  
196 metagenome assessed by shotgun sequencing. Samples are colored by group. C. Principal  
197 coordinates analysis of the BrayCurtis dissimilarities of study's participants day 14 microbiota  
198 metagenome assessed by shotgun sequencing. Samples are colored by group.

199

200 **Figure S8: Effect of carboxymethylcellulose consumption on the fecal metabolome.** Heatmap  
201 presenting day 14 participants fecal metabolome.

202  
203 **Figure S9: Effect of carboxymethylcellulose consumption on the fecal metabolome.** Evolution  
204 of fecal concentration of the various amino acids over the course of the study. Significance was  
205 determined using two-way ANOVA corrected for multiple comparisons with a Bonferroni post-  
206 test

207  
208 **Figure S10: Impact of CMC on AccQ•Tag-based detection of various amino acids.**  
209 Significance was determined using one-way ANOVA corrected for multiple comparisons with a  
210 Bonferroni post-test.

211  
212 **Figure S11: NMR-based detection of carboxymethylcellulose in fecal samples. A.**  
213 **Representative spectra obtained using feces from a control participant, feces from a CMC-treated**  
214 **participant, and CMC standard. B. Spectra obtained using various concentration of CMC (0.5, 1.0,**  
215 **2.0, 3.0 and 4.0 mg/ml). Each concentration was analyzed in triplicate. C. Standard curve obtained**  
216 **using CMC standard solutions and  $^1\text{H}$  NMR data (ppm 3.976-4.02). CMC integral data were**  
217 **normalized to the internal standard TSP.**

218  
219 **Figure S12: Effect of carboxymethylcellulose consumption on the urine metabolome. A.**  
220 **Heatmap presenting participants fecal metabolome over the course of the study. B. Heatmap**  
221 **presenting day 14 participants urine metabolome.**

222

223 **Figure S13: Effect of carboxymethylcellulose consumption on microbiota localization.** Effect  
224 of dietary emulsifier CMC consumption on microbiota localization (distance of the closest bacteria  
225 from the surface of the epithelium), measured both pre- and post- intervention, for each participants  
226 colored by group. Representative images are presented.

Journal Pre-proof

227 **Supplemental references**

- 228 1. Fedirko V, Tran HQ, Gewirtz AT, et al. Exposure to bacterial products lipopolysaccharide  
229 and flagellin and hepatocellular carcinoma: a nested case-control study. *BMC Med*  
230 2017;15:72.
- 231 2. Gilbert JA, Meyer F, Jansson J, et al. The Earth Microbiome Project: Meeting report of the  
232 "1 EMP meeting on sample selection and acquisition" at Argonne National Laboratory  
233 October 6 2010. *Standards in genomic sciences* 2010;3:249-53.
- 234 3. Caporaso JG, Lauber CL, Walters WA, et al. Ultra-high-throughput microbial community  
235 analysis on the Illumina HiSeq and MiSeq platforms. *The ISME journal* 2012;6:1621-4.
- 236 4. Bolyen E, Rideout JR, Dillon MR, et al. Reproducible, interactive, scalable and extensible  
237 microbiome data science using QIIME 2. *Nat Biotechnol* 2019;37:852-857.
- 238 5. Callahan BJ, McMurdie PJ, Rosen MJ, et al. DADA2: High-resolution sample inference  
239 from Illumina amplicon data. *Nat Methods* 2016;13:581-3.
- 240 6. McDonald D, Price MN, Goodrich J, et al. An improved Greengenes taxonomy with  
241 explicit ranks for ecological and evolutionary analyses of bacteria and archaea. *ISME J*  
242 2012;6:610-8.
- 243 7. Baym M, Kryazhimskiy S, Lieberman TD, et al. Inexpensive multiplexed library  
244 preparation for megabase-sized genomes. *PLoS One* 2015;10:e0128036.
- 245 8. Bushnell B. BBMap: A Fast, Accurate, Splice-Aware Aligner Lawrence Berkeley  
246 National Lab.(LBNL), Berkeley, CA (United States).  
247 <https://www.osti.gov/servlets/purl/1241166>. 2014.
- 248 9. Jiang H, Lei R, Ding SW, et al. Skewer: a fast and accurate adapter trimmer for next-  
249 generation sequencing paired-end reads. *BMC Bioinformatics* 2014;15:182.

- 250 10. Franzosa EA, McIver LJ, Rahnavard G, et al. Species-level functional profiling of  
251 metagenomes and metatranscriptomes. *Nat Methods* 2018;15:962-968.
- 252 11. Chassaing B, Koren O, Carvalho FA, et al. AIEC pathobiont instigates chronic colitis in  
253 susceptible hosts by altering microbiota composition. *Gut* 2014;63:1069-80.
- 254 12. Johansson ME, Hansson GC. Preservation of mucus in histological sections,  
255 immunostaining of mucins in fixed tissue, and localization of bacteria with FISH. *Methods*  
256 *in molecular biology* 2012;842:229-35.
- 257 13. Chassaing B, Koren O, Goodrich JK, et al. Dietary emulsifiers impact the mouse gut  
258 microbiota promoting colitis and metabolic syndrome. *Nature* 2015;519:92-6.
- 259 14. Chassaing B, Ley RE, Gewirtz AT. Intestinal epithelial cell toll-like receptor 5 regulates  
260 the intestinal microbiota to prevent low-grade inflammation and metabolic syndrome in  
261 mice. *Gastroenterology* 2014;147:1363-77 e17.
- 262 15. Jiang L, Huang J, Wang Y, et al. Eliminating the dication-induced intersample chemical-  
263 shift variations for NMR-based biofluid metabonomic analysis. *Analyst* 2012;137:4209-  
264 19.
- 265 16. Tian Y, Zhang L, Wang Y, et al. Age-related topographical metabolic signatures for the rat  
266 gastrointestinal contents. *J Proteome Res* 2012;11:1397-411.
- 267 17. Armenta JM, Cortes DF, Pisciotta JM, et al. Sensitive and rapid method for amino acid  
268 quantitation in malaria biological samples using AccQ.Tag ultra performance liquid  
269 chromatography-electrospray ionization-MS/MS with multiple reaction monitoring. *Anal*  
270 *Chem* 2010;82:548-58.
- 271 18. Krautkramer KA, Fan J, Backhed F. Gut microbial metabolites as multi-kingdom  
272 intermediates. *Nat Rev Microbiol* 2021;19:77-94.

- 273 19. Hosseinkhani F, Heinken A, Thiele I, et al. The contribution of gut bacterial metabolites in  
274 the human immune signaling pathway of non-communicable diseases. *Gut Microbes*  
275 2021;13:1-22.
- 276 20. Vernocchi P, Del Chierico F, Putignani L. Gut Microbiota Profiling: Metabolomics Based  
277 Approach to Unravel Compounds Affecting Human Health. *Front Microbiol* 2016;7:1144.  
278

Journal Pre-proof

**Table S2.** NMR data for the metabolites found in stool (S) and urine (U).

NO.	Metabolites	Moieties	$\delta$ $^1\text{H}$ (ppm)	$\delta$ $^{13}\text{C}$ (ppm)	Location	Source*
1	acetone	CH <sub>3</sub>	2.23(s) <sup>a</sup>	33.2	S	
2	butyrate	CH <sub>3</sub>	0.90(t)	16.3	S	microbial
		$\beta$ CH <sub>2</sub>	1.56(m)	21.5		
		$\alpha$ CH <sub>2</sub>	2.15(t)	42.7		
		COOH		186.8		
3	isoleucine	$\delta$ CH <sub>3</sub>	0.94(t)	14.2	S	
		$\gamma$ CH <sub>3</sub>	1.01(d)	17.7		
		$\gamma$ CH <sub>2</sub>	1.25(m)	27.5		
		$\gamma'$ CH <sub>2</sub>	1.48(m)	27.5		
		$\beta$ CH	1.98(m)	37.7		
		$\alpha$ CH	3.67(d)	62.4		
		COOH		177.1		
4	leucine	$\delta$ CH <sub>3</sub>	0.96(d)	24.5	S	
		$\delta$ CH <sub>3</sub>	0.97(d)	23.5		
		$\gamma$ CH	1.69(m)	27.3		
		$\beta$ CH <sub>2</sub>	1.71(m)	42.8		
		$\alpha$ CH	3.74(t)	56.4		
		COOH		178.3		
5	valine	$\gamma$ CH <sub>3</sub>	0.99(d)	19.6	S	
		$\gamma$ CH <sub>3</sub>	1.04(d)	20.7		
		$\beta$ CH	2.27(m)	32.0		
		$\alpha$ CH	3.62(d)	63.3		
		COOH		177.1		
6	propionate	CH <sub>3</sub>	1.06(t)	13.2	S	microbial
		CH <sub>2</sub>	2.19(q)	33.7		
		COOH		187.4		
7	lactate	CH <sub>3</sub>	1.33(d)	22.5	S, U	
		CH	4.11(q)	71.9		
8	alanine	COOH		185.3	S, U	
		$\beta$ CH <sub>3</sub>	1.48(d)	19.2		
		$\alpha$ CH	3.79(q)	53.4		
9	lysine	COOH		178.8	S	
		$\gamma$ CH <sub>2</sub>	1.48(m)	23.9		
		$\delta$ CH <sub>2</sub>	1.72(m)	29.4		
		$\beta$ CH <sub>2</sub>	1.90(m)	33.0		
		$\epsilon$ CH <sub>2</sub>	3.03(t)	42.2		
		$\alpha$ CH	3.76(t)	57.6		
10	acetate	COOH		177.5	S, U	microbial
		CH <sub>3</sub>	1.92(s)	26.2		
11	glutamate	COOH		184.2	S	
		$\beta$ CH <sub>2</sub>	2.10(m)	30.1		
		$\beta'$ CH <sub>2</sub>	2.09(m)	30.1		
		$\gamma$ CH <sub>2</sub>	2.36(m)	36.4		
		$\alpha$ CH	3.77(m)	57.6		

		C=O		184.0	
		COOH		177.5	
12	methionine	$\delta$ CH <sub>3</sub>	2.14(s)	16.8	S
		$\beta$ CH <sub>2</sub>	2.16(m)	33.2	
		$\gamma$ CH <sub>2</sub>	2.65(t)	31.6	
		$\alpha$ CH	3.86(m)	56.9	
		COOH		176.6	
13	succinate	CH <sub>2</sub>	2.41(s)	37.6	S, U
		COOH		184.4	
14	citrate	CH <sub>2</sub>	2.54(d)	46.5	U
		'CH <sub>2</sub>	2.66(d)	46.5	
		C-OH		76.4	
		COOH		181.5	
		COOH		183.9	
15	aspartate	$\beta$ CH <sub>2</sub>	2.68(m)	39.5	S
		$\beta'$ CH <sub>2</sub>	2.82(m)	39.5	
		$\alpha$ CH	3.91(m)	55.3	
		$\beta$ COOH		180.5	
		$\alpha$ COOH		176.9	
16	asparagine	$\beta$ CH <sub>2</sub>	2.86(dd)	37.6	S
		$\beta'$ CH <sub>2</sub>	2.96(dd)	37.6	
		$\alpha$ CH	4.00(m)	54.3	
		C=O		177.1	
		COOH		176.3	
17	dimethylamine (DMA)	CH <sub>3</sub>	2.72(s)	39.4	U
18	creatine	CH <sub>3</sub>	3.04(s)	40.0	S
		CH <sub>2</sub>	3.93(s)	57.1	
		C=NH		159.4	
		COOH		177.2	
19	choline	N(CH <sub>3</sub> ) <sub>3</sub>	3.21(s)	56.8	S, U
		NCH <sub>2</sub>	3.52(m)	58.5	
		OCH <sub>2</sub>	4.07(m)	70.2	
20	taurine	CH <sub>2</sub> SO <sub>3</sub>	3.25(t)	50.7	S, U
		NCH <sub>2</sub>	3.43(t)	38.5	
21	glycine	CH <sub>2</sub>	3.57(s)	44.6	S, U
		COOH		175.2	
22	$\alpha$ -glucose	4CH	3.42(dd)	72.7	S
		2CH	3.54(dd)	74.9	
		3CH	3.73(dd)	76.2	
		5CH	3.83(dd)	74.4	
		6CH <sub>2</sub>	3.83(dd)	63.7	
		1CH	5.24(d)	95.4	

23	$\beta$ -glucose	2CH	3.26(dd)	77.5	S			
		4CH	3.40(dd)	72.9				
		5CH	3.47(dd)	79.0				
		3CH	3.50(dd)	79.0				
		6CH	3.74(dd)	63.7				
		6CH'	3.90(dd)	63.9				
		1CH	4.45(d)	99.3				
24	uracil	CH	5.81(d)	103.9	S			
		CH	7.54(d)	146.5				
		C=O		170.6				
		C=O		155.9				
25	fumarate	CH	6.53(s)	138.1	S			
		COOH		179.2				
26	tyrosine	$\beta$ CH <sub>2</sub>	3.06(dd)	38.3	S			
		$\beta'$ CH <sub>2</sub>	3.15(dd)	38.3				
		$\alpha$ CH	3.94(dd)	59.2				
		3 or 5CH	6.91(d)	118.8				
		2 or 6CH	7.20(d)	132.4				
		C(ring)		129.4				
		C-OH(ring)		157.7				
		COOH		177.1				
27	tryptophan	$\beta$ CH <sub>2</sub>	3.31(dd)	29.5	S			
		$\beta'$ CH <sub>2</sub>	3.49(dd)	29.5				
		$\alpha$ CH	4.06(dd)	58.5				
		5CH	7.21(t)	122.5				
		6CH	7.29(t)	125.0				
		2CH	7.33(s)	128.2				
		7CH	7.55(d)	114.9				
		4CH	7.74(d)	121.5				
				COOH			177.4	
				$\beta$ CH <sub>2</sub>		3.13(dd)	38.4	S
28	phenylalanine	$\beta'$ CH <sub>2</sub>	3.29(dd)	38.4				
		$\alpha$ CH	3.98(dd)	59.3				
		2 or 6CH	7.33(m)	130.7				
		4CH	7.38(m)	131.9				
		3 or 5CH	7.43(m)	132.0				
		C(ring)		139.4				
		COOH		176.4				
29	histidine	$\beta$ CH <sub>2</sub>	3.14(dd)	30.8	S			
		$\beta'$ CH <sub>2</sub>	3.25(dd)	30.8				
		$\alpha$ CH	3.99(dd)	58.7				
		5CH	7.08(s)	120.1				
		3CH	7.83(s)	138.3				
		C(ring)		133.6				
		COOH		176.4				
30	formate	CH	8.45(s)	172.4	S			

31	hypoxanthine	8CH	8.20(s)	145.6	S	
		6CH	8.22(s)	149.2		
32	inosine	CH <sub>2</sub>	3.85(dd)	63.8	S	
		'CH <sub>2</sub>	3.92(dd)	63.8		
		5H'	4.28(q)	88.6		
		4H'	4.44(t)	73.4		
		2H'	6.10(d)	91.4		
		8H	8.24(s)	150.1		
		2H	8.34(s)	143.3		
33	xanthine	8CH	7.89(s)	144.0	S	
34	uridine	CH <sub>2</sub>	3.81(d)	64.3	S	
		'CH <sub>2</sub>	3.92(d)	64.3		
		4H'	4.14(q)	86.6		
		3H'	4.24(t)	73.1		
		2H'	4.36(t)	78.0		
		5H	5.90(d)	95.2		
		6H	5.91(d)	90.8		
		1H'	7.87(d)	144.1		
35	creatinine	CH <sub>3</sub>	3.05(s)	33.2	U	
		CH <sub>2</sub>	4.06(s)	59.2		
36	trimethylamine oxide (TMAO)	N- N-CH <sub>3</sub>	3.27(s)	62.5	U	microbial
37	hippurate	αCH <sub>2</sub>	3.97(s)	47.2	U	
		3 or 5 CH	7.56(dd)	132.1		
		4CH	7.64(t)	135.5		
		2 or 6 CH	7.83(dd)	130.2		
		NH	8.56(brs)			
		C=O		173.3		
		COOH		180.0		
38	phenylacetylglycine (PAG)	CH <sub>2</sub>	3.65(s)	45.2	U	
		2 or 6 CH	7.36(m)	132.0		
		4CH	7.36(m)	119.3		
		3 or 5 CH	7.42(m)	132.0		
		C=O		167.8		
39	p- hydroxyphenylacetate	CH <sub>2</sub>	3.45(s)	46.9	U	microbial
		2 or 6 CH	6.87(d)	118.2		
		3 or 5 CH	7.16(d)	133.4		
		C-OH		156.9		
		COOH		182.7		
40	indoxyl sulfate	5CH	7.20(m)	123.0	U	microbial
		6CH	7.27(m)	125.2		
		2CH	7.36(s)	118.7		
		7CH	7.50(m)	115.0		
		4CH	7.70(m)	120.3		

41	1-methylnicotinamide	CH <sub>3</sub>	4.48(s)	51.3	U
		5CH	8.18(m)	130.9	
		4CH	8.89(dt)	146.4	
		6CH	8.96(m)	150.0	
		2CH	9.27(m)	147.9	
42	<i>scyllo</i> -inositol	CHOH	3.35(s)	74.3	U

<sup>a</sup> s, singlet; d, double; t, triplet; q, quartet; m, multiplet; dd, double of doubles; dt, double of triplet.

\*Only the microbial metabolic products are indicated. Other metabolites have more complicated sources <sup>18-20</sup>.

18. Krautkramer KA, Fan J, Backhed F. Gut microbial metabolites as multi-kingdom intermediates. *Nat Rev Microbiol* 2021;19:77-94.
19. Hosseinkhani F, Heinken A, Thiele I, et al. The contribution of gut bacterial metabolites in the human immune signaling pathway of non-communicable diseases. *Gut Microbes* 2021;13:1-22.
20. Vernocchi P, Del Chierico F, Putignani L. Gut Microbiota Profiling: Metabolomics Based Approach to Unravel Compounds Affecting Human Health. *Front Microbiol* 2016;7:1144.